UNIVERSITA' DI NAPOLI FEDERICO II

DOTTORATO DI RICERCA
BIOCHIMICA E BIOLOGIA CELLULARE E MOLECOLARE
XXV CICLO

Gene expression pattern of relaxins and their receptors in *Danio rerio*

Candidate
Marcella Fiengo

Tutor
Prof. Francesco Aniello

Coordinator
Prof. Paolo Arcari

Co-Tutor
Dr. Aldo Donizetti

Academic Year 2011/2012

SUMMARY

The relaxin (RLN) peptides exert different biological effects ranging from reproduction to regulating central nervous processes. Until now, few studies have been performed in embryonic development and in vertebrate models beyond mammals. I used zebrafish, as experimental model, to characterize the spatial and temporal expression pattern of the relaxin/receptor system in vertebrate embryogenesis. In previous analysis, the expression pattern of the zebrafish *rln3*a and *rln3*b paralogue genes was characterized. These paralogue genes are expressed in periaqueductal gray and nucleus incertus, showing a conserved expression pattern during vertebrate evolution. In this thesis, I demonstrated that another member of zebrafish relaxin family, the *rln*, is express in many brain areas of zebrafish embryo. In particular, I showed that the *rln* transcript co-localized with *rln3a* in the putative nucleus incertus (NI). The *rln* gene expression in many developing brain regions is in line with the phylogenetic analysis, which suggests that teleost *rln* gene is closely related to *rln3-like* ancestor gene. The *insl-5*a and *insl-5*b paralogue genes showed their expression localized in two distinct cellular types of intestinal epithelium. My data showed that the *insl5* expression pattern is conserved from fish to mammals, since the human INSL5 gene is expressed in the intestinal tissue; in addition, they showed that a sub-functionalization event likely differentiated the gene expression regulation of the two zebrafish paralogue genes. Beyond the ligands, I extend the gene expression characterization to the relaxins receptors encoding genes. I demonstrated that the zebrafish *rxfp1* gene has the same syntenic genomic organization, and a similar exon-intron structure to the human homologue gene. Furthermore, the deduced Rxfp1 protein sequence shows a high degree of amino acid similarity when compared with the human protein and the conservation of all amino acid identity necessary for the binding with relaxin. The *rxfp1* expression pattern in *Danio rerio* embryos is very similar to that reported in the adult mammalian brain, suggesting a pivotal role of this receptor in the neurophysiology processes already at very early developmental stages. Only one of three *rxfp2* paralogue gene is expressed during embryonic developmental stage and its transcript is localized in pineal gland, habenula and preoptic area. The analysis of

rxfp3 paralogue genes expression pattern showed that they are differentially expressed both in neural tissues and non-neural territories. I showed that, in embryonic development, the different expression areas of relaxin receptors and probably their function are conserved between mammals and fishes. Overall, my data provided evidence that the relaxin/receptor system is active during zebrafish embryogenesis, and that their expression territories and probably their function are conserved between mammals and fishes.

RIASSUNTO

Le relassine sono ormoni peptidici che esercitano svariati effetti biologici sulla riproduzione e sui processi neurali. Lo studio della famiglia delle relassine e dei rispettivi recettori si è incentrato principalmente su organismi adulti e su modelli sperimentali di specie mammifere. Al contrario, pochi dati sono disponibili sul ruolo svolto durante l'embriogenesi ed in organismi diversi dai mammiferi. Per il mio progetto di dottorato, ho usato come modello sperimentale *Danio rerio,* comunemente noto come pesce zebra, al fine di allargare la conoscenza sul sistema relassina/recettore durante l'embriogenesi dei vertebrati.
Analisi precedenti effettuate nel laboratorio dove ho svolto il mio lavoro di ricerca, hanno dimostrato che, durante lo sviluppo embrionale, i geni paraloghi di uno dei membri della famiglia delle relassine, *rln3*a e *rln3*b, sono entrambi espressi nel cervello di zebrafish, in una regione omologa al nucleo incerto dei mammiferi. Nel mio lavoro di tesi, ho ampliato l'analisi agli altri membri della famiglia delle relassine ed ai rispettivi recettori. La caratterizzazione del gene *rln* ha mostrato che, la sequenza amminoacidica possiede un'elevata percentuale d'identità con i due paraloghi *rln3*a e *rln3*b del pesce zebra, avvalorando l'ipotesi che l'intera famiglia delle relassine si sia evoluta da un unico gene ancestrale *rln3-simile*. Il gene *rln* è espresso nel sistema nervoso centrale ed il suo trascritto co-localizza con il gene *rln3*a nel putativo nucleo incerto. Nell'insieme i territori di espressione del gene *rln* nel pesce zebra, comparati a quelli del ratto, fanno ipotizzare un ruolo nei processi neuroendocrini e sensoriali, conservato nell'evoluzione dei vertebrati. Inoltre, la presenza del trascritto a livello della regione pancreatica e della tiroide, fa supporre una funzione di Rln come ormone endocrino e paracrino. I territori di espressione dei due paraloghi *insl5*a e *insl5*b sono anch'essi conservati durante l'evoluzione, essendo entrambi espressi a livello dell'intestino come per i mammiferi. Inoltre, data la loro espressione in tipi cellulari differenti, si è ipotizzato un processo di sub-funzionalizzazione dei due geni paraloghi. Le relassine interagiscono con una classe di recettori accoppiati a proteine G (GPCR), noti come RXFP. In seconda analisi, la mia attività di ricerca si è focalizzata sulla caratterizzazione dei profili di espressione genica di tali recettori. L'omologo nel pesce

zebra del recettore RXFP1 mostra un elevato livello di conservazione sia nella struttura del gene che nella sequenza amminoacidica. Anche i territori di espressione risultano conservati nell'evoluzione dei vertebrati, suggerendo un ruolo centrale di questo recettore nei processi neurali già nelle prime fasi di vita di un organismo. RXFP2 presenta 3 omologhi nel pesce zebra, ma solo uno di essi risulta espresso durante lo sviluppo embrionale, a partire dallo stadio larvale. L'espressione genica è stata rivelata in territori come l'epifisi, l'abenula e l'area preottica, strutture correlate al controllo degli stati emotivi ed al ritmo circadiano. RXFP3 e RXFP4 sono i recettori che presentano una situazione più complessa nel pesce zebra, infatti nel suo genoma sono presenti 7 geni omologhi, di cui solo alcuni di essi sono espressi durante lo sviluppo embrionale. L'analisi di localizzazione dei rispettivi mRNA, ha mostrato che l'espressione di tali geni riguarda strutture nervose coinvolte nell'elaborazione somato-sensoriale e nella regolazione neuroendocrina, come già noto per il cervello di ratto adulto. Presi nel loro insieme i dati di espressione degli omologhi di RXFP3 e RXFP4 nel pesce zebra, fanno ipotizzare che probabilmente i meccanismi di regolazione dell' espressione genica e la loro funzione ricapitolano i territori di espressione e la funzione dei soli due geni presenti nel genoma dei mammiferi. Nel complesso, i dati ottenuti nel mio lavoro di tesi mostrano che il sistema ligando/recettore delle relassine è attivo durante l'embriogenesi, e che i loro territori di espressione e, probabilmente, la loro funzione nell'embrione sono conservati tra mammiferi e pesci.

Index

2.0 Introduction……..……...1-12

2.1 The relaxin family: structure and evolution ……..…..1-5

2.2 The ligands……...5-7
.
2.3 The relaxin receptor…….....……..7-10

2.4 Aim ……11-12

3.0 Materials and Methods……...…….…....13-20

3.1 Experimental model…….13-14

3.2 Animals …….…...14

3.3 Database rearch and sequence analysis……..…...14

3.4 RNA extraction and clean up RNA ……..……14

3.5 cDNA syntesis…….14-15

3.6 Polimerase chain reaction (PCR) and quantitative Real Time PCR (qPCR)……...15-16

3.7 Cloning in pGEM®-T Easy Vector…….....17-18

3.8 RNA Probes for in situ hybridization experiments ……..18

3.9 Whole mount embryo in situ hybridization ……18-19

3.10 *in situ* hybridization on zebrafish adult tissues. …….....20

4.0 Results ……....21-50

4.1 relaxin ligands.....21-32

4.12a *relaxin* ……..……..21-27

4.1b *insl-5*a and *insl-5*b……..... 28-32

4.2 Relaxin receptors.....32-50

4.2a *rxfp1*……...32-39

4.2b *rxfp2* ……..39-41

4.2c *rxfp3* ……...……...41-50

5.0 Conclusion…….……...……...51-58

6.0 References ……..…….....59-67

List of Tables and Figures:

Table 1: Primers for PCRs……...16-17

Table2: Proteinase K times for each zebrafish embryonic stage…….…….....19

Table3: Summary of relaxin ligands and receptors embryonic expression pattern analysed by RT-PCR and qRT-PCR experiments…….53

Table 4: Summary of relaxin ligands and their cognate receptors expression territories analysed by in situ hybridization experiments…….58

Figure 1. Diagrammatic structure of the relaxin ……...….....2

Figure 2. Evolutionary model of vertebrate relaxin genes……...…4

Figure 3. Evolutionary model of vertebrate receptor genes…….....5

Figura 4. Ligand–receptor relationships……..…8

Figura 5. Comparative analysis of *rln* amino acid sequence and gene structure…….22

Figure 6. Expression pattern of the rln gene by RT-qPCR……...….24

Figure 7. Localization of the *rln* transcript by whole mount *in situ* hybridization……..27

Figure 8. Expression pattern of the paralogs gene *insl-5*a and *insl-5*b RT-qPCR……...29

Figure 9. Whole mount *in situ* hybridization for *insl-5*a and *insl-5*b transcript……....30

Figure 10. Histological intestine cross section of adult zebrafish intestine tissue for *insl-5a* transcript…….31

Figure 11. Histological intestine cross section of adult zebrafish intestine tissue for *insl-5*b transcript…….32

Figure 12. Amino acid alignment of the human RXFP1 and zebrafish *Rxfp1*……..34

Figure 13. Schematic representation of the human RXFP1 and zebrafish *rxfp1*……...36

Figure 14. Temporal expression pattern of zebrafish *rxfp1* by RT–PCR experiments……...37

Figure 15. *In situ* localization of *rxfp1* transcript……...……..39

Figure 16. Temporal expression pattern of zebrafish *rxfp2* paralogue genes by RT– PCR experiments……40

Figure 17. Whole mount *in situ* hybridization of *rxfp2-like* gene.....41

Figure 18. Temporal expression pattern of zebrafish *rxfp3 paralogue genes* by RT–PCR experiments……42

Figure 19. Whole mount *in situ* hybridization experiments for *rxfp3*-1 transcript……43

Figure 20. Whole mount *in situ* hybridization for *rxfp3-2*a transcript……..…..……46

Figure 21. Trasversal section of whole mount *in situ* hybridization for *rxfp3-2*a transcript……47

Figure 22. Whole mount *in situ* hybridization for *rxfp3-3*b transcript……....49

Figure 23. Trasversal section of whole mount *in situ* hybridization for *rxfp3-3*b transcript…....……50

2.0 INTRODUCTION

2.1 *The relaxin family: structure and evolution*

The members of relaxin/insulin-like peptide family are encoded by seven genes in humans and are all structurally related to insulin. In particular, the peptide family is made of three relaxin genes (RLN1, RLN2 and RLN3) and four insulin-like (INSL) peptide genes (INSL3, INSL4, INSL5 and INSL6). Relaxin (RLN2), the first identified family member (Hisaw, 1926), was recognized as a hormone influencing the reproduction during normal pregnancy and parturition in many mammalian species (reviewed in Bathgate et al., 2006). Currently, it is known that RLN is involved in a broad range of reproductive and neuroendocrine functions (Bathgate et al., 2006). The relaxin family and insulin family belong to the insulin/relaxin superfamily. The two families diverged early in vertebrate evolution to form the relaxin peptide family, which includes several signalling molecules that share similar secondary structures (Olinski et al., 2006 a/b). All members are synthesized as a pre-prohormone consisting of a signal peptide, B-domain, C-peptide, and A-domain (Ivell and Einspainer, 2002). In particular, like all other secreted peptide hormones, relaxin is synthesized first as a pre-pro-peptide, with the N-terminal pre- or signal sequence useful for the hormone secretion. The nascent pro-polypeptide is sequestered into the lumen of the endoplasmic reticulum of the hormone producing cells. The cleavage of the C peptide *in vivo* produces a mature peptide heterodimer of A- and B-chains linked by two inter-chain and one intra-chain disulphide bonds, between the six highly conserved cysteine residues in the A and B chains (Marriott et al., 1992). The C-chain facilitates the folding of the protein and the formation of the three disulphide bridges and it is biologically active in the rat central nervous system acting as an independent signalling molecule (Brailoiu et al., 2009) (Figure. 1). Although they are structurally related to insulin, the relaxin family peptides produce their physiological effects by activating a group of four G protein coupled receptors (GPCRs), relaxin family peptide receptors 1–4 (RXFP1–4).

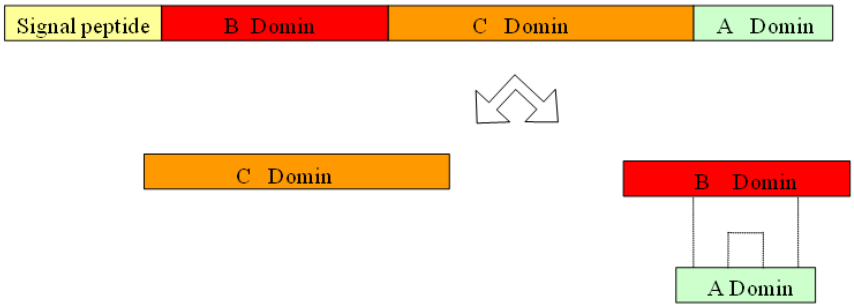

Figure. 1: **Diagrammatic structure of the precursor protein generated from the transcript of relaxin.** Scheme shows the intracellular enzymatic processing of pre-pro-relaxin into its final products.

The relaxin ligands and their receptors were also analysed from an evolutionary perspective, in order to understand how this signalling system evolved in vertebrates. Relaxins form together with insulins a unique superfamily, whose members arose from a single ancestor gene in chordate lineage (Olinski et al., 2006a; Olinski et al., 2006b). Although these ligands display relatively low primary amino-acid sequence identity, phylogenetic analyses indicate that they evolved from a common ancestor RLN3-like gene (Hsu et al., 2003; Hsu et al., 2005; Wilkinson et al., 2005b; Good et al., 2012). After the two rounds of whole genome duplications occurred in vertebrate lineage, one single ancestor generated three relaxin genes (a fourth was lost). One of these copies underwent a further duplication leading to a total of four gene copies before tetrapods and teleosts divergence (Olinski et al., 2006a; Good-Avila et al., 2009). Analyses of whole genome sequence data have confirmed that three rounds of whole genome duplication (WGD) have contributed immensely to the diversification of vertebrates (Abi-Rached et al., 2002; Dehal et al., 2005); two rounds of WGD (2R) occurred in early vertebrate evolution, while the third round (3R) occurred at the base of the teleostean lineage. It has been proposed that the major vertebrate novelties, such as their structurally complex nervous, immune and reproductive systems, arose as a result of the massive amplification of genes that occurred during WGD. Indeed, the diversification of RLN/INSL and RXFP

(Relaxin Family Peptide Receptors) genes was coincidental with 2R events, suggesting that they probably played an important role in the establishment of neuroendocrine and reproductive regulation in early vertebrate evolution. In addition, it has been observed that the teleost-specific 3R, strongly contributed to the genetic richness of teleosts and their biological success (Hoegg et al., 2004; Mayer et al., 2005; Yegorov et Good., 2012). The syntenic data analysis showed that in teleost species, the six copies of relaxin family sequences are linked to four loci: two loci are syntenic to human INSL5 (Park et al., 2008), and harbour teleost *insl5a* and *insl5b*; a locus syntenic to the human relaxin cluster contains teleost *rln;* the locus syntenic to human RLN3 contains *rln3a* and *rln3b,* and the locus syntenic to human INSL3 contains teleost *insl3* (Figure. 2). Thus, four genes were present in the common ancestor of humans and teleosts. Of the six relaxin family genes in teleosts, two arose as a result of the fish specific WGD. On the contrary, in mammals, the RLN gene duplicated to give rise to two additional members of the family, INSL4 and INSL6. In addition, in a more recent duplication of the *RLN* gene, specific to humans and anthropoid apes, resulted in two copies of RLN in primates, called RLN1 and RLN2, with RLN2 being functionally equivalent to the RLN in other mammals (Good Avila et al., 2009).

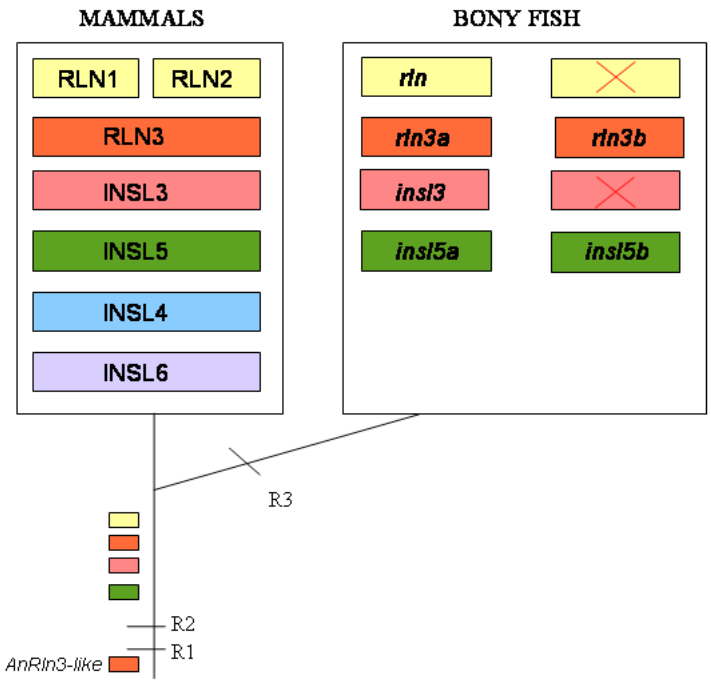

Figure. 2: **Evolutionary model of vertebrate relaxin genes in relation to the three rounds of whole genome duplication events (R1-3)**. X indicate pseudogenes or lost genes.

On the basis of ligand/receptor co-evolution, it was initially expected that relaxin receptors should have been tyrosine kinase receptors as for insulins, but, surprisingly, they belonged to two unrelated and large evolutionarily distant groups of GPCRs, the RXFP1/2 and RXFP3/4. It was proposed that the signalling of the ancestral RLN/INSL peptide in the chordate ancestor occurred via RXFP1/2-type receptors. Only at the onset of 2R, the RXFP3/4-type receptor was recruited to produce a signalling system encoded by 3 genes (2 receptors and a single ligand). It is tempting to hypothesize that this ancestral 2-receptor system had a dual function and played roles in both reproductive (using RXFP1/2-type receptor) and neuroendocrine processes (via RXFP3/4-type receptor) (Yegorov et al., 2012). Then, during evolution, only those genes potentially involved in neuroendocrine

regulation (as *rln*3, *insl*5 and half of the *rxfp3/4*-type cognate receptors) were retained after 3R in teleosts. The post-3R retention of *rln*3 and *insl*5 paralogues was paralleled by the retention of duplicates of *rxfp3*-2 and *rxfp3*-3, suggesting both co-functioning and sub-functionalization of their neuroendocrine roles (Good et al., 2012) (Figure. 3).

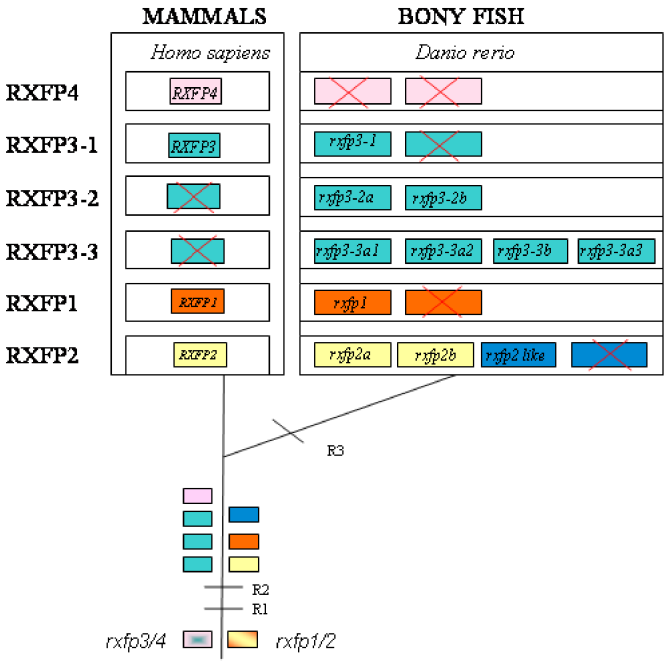

Figure. 3: **Evolutionary model of vertebrate receptor genes in relation to the three rounds of whole genome duplication events (R1-3).** X indicate pseudogenes or lost genes.

2.2 The ligands

Only for a limited number of these peptides their physiological effects have been defined. Although RLN was initially identified for its influence on parturition, its roles has now been recognized in a number of physiological systems including cardiovascular, renal and reproductive systems, in fibrosis and allergic responses (Schwabe, 2000; Bathgate et al., 2002a, 2006a).

Relaxin-3 emerged prior to the divergence of fish and it is considered as the 'ancestral' member of the relaxin peptide family. The relaxin-3 gene is highly conserved across fish, frogs, rodents and primates, suggesting that the peptide performs important physiological functions (Bathgate et al., 2002b; Wilkinson et al., 2005a; Callander and Bathgate, 2010). The RLN3 gene is mainly expressed in a restricted area of rat, mouse and monkey brain, known as "nucleus incertus" (NI), although some scattered RLN3-expressing cells in different brain areas were also revealed (Bathgate et al., 2002a; Burazin et al., 2002; Tanaka et al., 2005; Ma et al., 2007; Smith et al., 2010). Several functions of RLN3 have been suggested by studies on nucleus incertus. This neural cell cluster has been emerging as a key element of neural circuits regulating different processes such as arousal, stress and memory, exploratory navigation, defensive and ingestive behaviors, and responses to neurogenic stressors (Goto et al., 2001, 2005; Ryan et al., 2011; Olucha-Bordonau et al., 2011). In rodents, it has been shown that RLN3 is involved in food intake, stress responses and spatial memory (McGowan et al., 2005, 2006; Tanaka et al., 2005; Hida et al., 2006; Ma et al., 2009). Interestingly, the expression pattern of the RLN-3 gene is conserved during vertebrate evolution. Indeed, analysis of *rln3*a gene expression during zebrafish embryogenesis showed that the gene is expressed in a region likely homologous to the mammalian NI (Donizetti et al., 2008). The analysis of the zebrafish paralogue gene *rln3*b, evidenced that both genes were actively transcribed during embryogenesis and in the adult tissues. In addition, the expression pattern analysis evidenced remarkable differences between the two genes, likely as a consequence of a sub-fuctionalization process, where the ancestral expression pattern was partitioned between the two paralogues (Donizetti et al., 2009). For instance, during embryogenesis only *rln3*b is expressed during gastrulation, while only *rln3*a is expressed in the NI at the larval stage; in the adult organs, both genes are highly expressed in the brain but only *rln3*b showed remarkable expression in the testis (Donizetti et al., 2009).

INSL-3 function has been strictly linked to reproduction, in fact, in females, it has been shown to be involved in oocyte maturation and germ cells survivor, while in male, is involved in descentus scrotalis process (Nef et al., 1999; Zimmermman et al., 1999).

INSL-5 is expressed in human rectal and colon tissues and is likely involved in both appetite stimulation and colon motility (Conklin et al., 1999).
Very little information are available regarding INSL4–6.

2.3 The relaxin receptors

RLN/INSL peptides interact with two very dissimilar classes of G protein-coupled receptors (GPCRs), named RXFP1, RXFP2, RXFP3 and RXFP4. Two receptors, LGR7 (renamed RXFP1, Hsu et al., 2002) and LGR8 (renamed RXFP2, Kumagai et al., 2002), are leucine-rich-repeat containing GPCRs (LGR) and belong to the glycoprotein receptor cluster. This cluster of receptors contains three distinct LGR subgroups (type A, B and C), which have been defined based on different number of LRR motifs, the absence or presence of a LDLa motif (low density lipoprotein receptor like cysteine-rich motif) and the type-specific hinge region. The RXFP1 and RXFP2 belongs to the LGR family class C and are characterized by the presence of a LDLa motif at protein N-terminus followed by a very short hinge region and 10 LRR regions (Hsu et al., 2002). On the contrary, RXFP3 and RXFP4 (also known as SALPR or GPCR135 and GPCR142) are typical class A neuropeptide receptors and belong to the chemokine receptor cluster of the γ Group Rhodopsin family (based on GRAFS classification, Fredrikkson et al., 2003). Signalling pathways of RXFP3/RXFP4 result in the inhibition of adenylate cyclase and decrease in cAMP accumulation (Liu et al., 2003a/b, 2005b). In contrast, the stimulation of RXFP1 and RXFP2 results in the activation of adenylate cyclase and increase in cAMP level.
Currently, it is known that there is cross-reactivity between the relaxin peptides and their receptors (Good, 2012), with the exception of INSL3 and RXFP2, which *in vivo* represent an exclusive hormone-receptor pair (Bogatcheva et al., 2003; Bathgate et al, 2006; Halls et al., 2007). RXFP1 can be activated by both human RLN and H1-RLN, as well as by RLN3. Similarly, RXFP3 can be activated by both RLN3 and RLN, and to a lesser extent by INSL5. RXFP4 is activated mainly by INSL5, although can also cross-react with RLN3, but not with RLN, nor, of course, with INSL3 (Figure. 4) (Liu et al., 2005; Haugaard-Jonsson et al., 2009; Hossain et al., 2008).

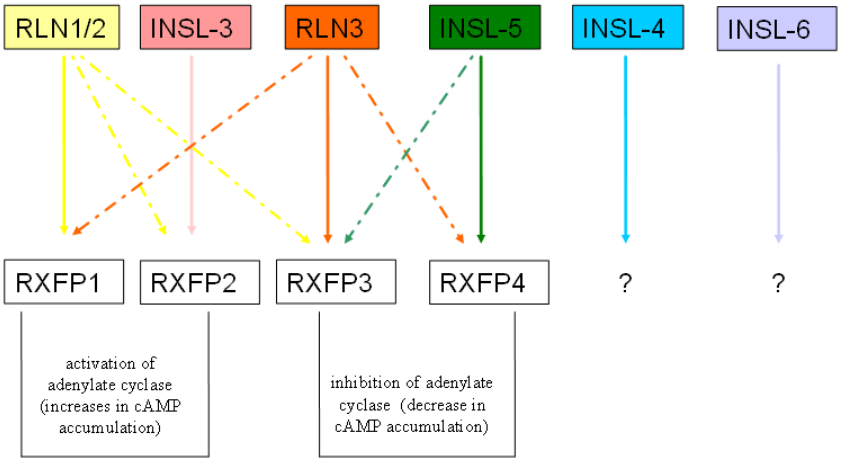

Figure. 4: **Ligand–receptor relationships for the relaxin-family peptides and their cognate receptors in Mammals.** The thickness of the arrows reflects the affinity and specificity of the interaction and their secondary response.

RXFP1 has been shown to be expressed in the reproductive organs, paralleling its role as the receptor for relaxin. In humans, RXFP1 mRNA has been found in the ovary (Hsu et al., 2002), uterus (Hsu et al., 2002; Luna et al., 2004; Mazella et al., 2004), placenta, testis and prostate (Hsu et al., 2002). A similar distribution has been shown in rodents (Hsu et al., 2000; Scott et al., 2004; Krajnc-Franken et al., 2004; Kubota et al., 2004). In addition, in relation to relaxin's autocrine/paracrine roles, RXFP1 mRNA has been found in the brain, kidney, heart, lung, liver, adrenal, thyroid and salivary glands, muscle, peripheral blood cells (Hsu et al., 2002).
As expected, RXFP2 is expressed in the fetal gubernaculum of male rats (Kubota et al., 2002) and mice (Overbeek et al., 2001) in accordance with its function as the receptor for INSL3. Additionally, RXFP2-KO mice (Gorlov et al., 2002) share the same cryptorchid phenotype as the INSL3-KO mice (Nef and Parada, 1999; Zimmermann et al., 1999). In the adult, RXFP2 is expressed in post-mitotic male germ cells, where it may have a role as a germ cell

survival factor (Kawamura et al., 2004; Anand-Ivell et al., 2006), and in Leydig cells and epididymis (Anand-Ivell et al., 2006). Additionally, in humans, RXFP2 mRNA has been shown to be expressed in the kidney, thyroid gland, muscle, uterus, peripheral blood cells, testis, brain and bone marrow (Hsu et al., 2002).

The RXFP3 gene expression was analysed by reverse transcriptase-PCR in different tissues. The expression is restricted to the brain and testis of rodents, which is very similar to the tissue expression pattern of the human RXFP3, which is also expressed in thymus, and adrenal gland (Liu et al., 2003). In rodents brain, the RXFP3 receptor has been localized in some sensory areas of the brain as the olfactory bulb, sensory cortex, amygdale, thalamus, inferior and superior colliculus, supraoptic nucleus, thalamic nuclei (paraventricular and centromedial), the dentate gyrus of the hippocampus, dorsal raphe, medial habenula and cortical fields (Boels et al., 2004; Liu et al., 2004; Smith et al., 2010). This RXFP3 neural network overlapped the regional distribution of RLN3. This is a further evidence for the interaction between RLN3 and RXFP3 and for the ability of RLN3/RXFP3 signaling to modulate “behavioral state” and an array of circuits involved in arousal, stress responses, affective state, and cognition (Smith et al., 2010).

RXFP4 gene is expressed in the mouse brain and testis, similarly to the human homologue, while in rats and dogs both RXFP4 and INSL5 are pseudogenes. In addition, in humans, the RXFP4 transcript has been detected in a broader range of tissues as kidney, lung, and spleen (Liu et al., 2005).

In teleosts, many more genes have been identified for both ligands and their receptors. It has been supposed that R*ln3b* is the cognate ligand of *Rxfp3-1*, while *Rln3*a has specialized to function with two receptors, namely, *Rxfp3-2*a and *Rxfp3-2*b. *Rxfp3-3a*1*, Rxfp3-3a*2*,* and *Rxfp3-3*b are candidate receptors for *insl5*a, while *Rxfp3-4* is the receptor for *insl5*b; in zebrafish, the loss of *rxfp4* was compensated by the gain of *rxfp3-3a*3, which could interact with *insl-5*b*; rxfp2*a and *rxfp2*b are considered the receptors for *insl-3; rxfp2-like* and *rxfp1* are considered the receptors for *rln*. Although for the circulating hormones we can, probably, disregard the promiscuous activation of other receptors at high ligand concentration, this may not be true for autocrine/paracrine relationships in the vicinity of sites of local synthesis, where local hormone concentrations can be very high. It is also important to recognize that although some circulating hormone concentrations can be quite low, most of these receptors can be activated, although briefly, by concentrations of ligand as low as that of their specific ligand, or even by concentrations in the subpicomolar range (Halls and Cooper, 2010; Ivell et al., 2009).

1.4 Aim

Studies in mammals evidenced an intricate ligand-receptor relationship for relaxins system. Great advantages might result from studies on relaxin system in non-mammalian model organisms. Moreover, most of relaxin/receptor system studies have been performed in adult mammalian organisms, whereas little is known about relaxin function during vertebrate embryogenesis.
Among experimental models, the *Danio rerio*, also called zebrafish, has emerged as one of the most useful in many research areas and particularly for embryonic development. By using zebrafish as experimental model, previous studies carried out in the laboratory of Prof. Aniello, provided several interesting insights on relaxin system. In particular, they showed that the *rln3a/b* paralogue genes, are differentially expressed in two territories of the developing zebrafish brain. In addition, these data provided, for the first time, the evidence of the nucleus incertus existence in fish, and supported the idea of an ancestral function for Rln3 peptide as a neurotransmitter. (Donizetti et al., 2008, 2009).
Recent phylogenetic analysis showed that the numerous vertebrate RLN/INSL and RXFP genes are the consequence of three rounds of whole genome duplication (WGD). Diversification of the relaxin system was driven primarily by whole genome duplications (WGD, 2R and 3R) followed by almost complete retention of the ligand duplicates in most vertebrates but massive loss of receptor genes in tetrapods. For receptor, the same phylogenetic reconstruction led to hypothesize that there was one ancestral gene for *rxfp3/4* and one for *rxfp1/2*, with differential reduction and expansion of gene repertoire occurred independently in the tetrapod and teleost lineages (Yegorov and Good, 2012).
In order to obtain more data on relaxin/receptor system function in vertebrate, and in particular, during embryonic development, the aim of this dissertation is the temporal and spatial characterization of relaxin ligand receptor gene expression during zebrafish embryonic development. The experimental data will be discussed in comparison with the data reported in literature for the mammalian relaxin ligand/receptor system. This will provide new insights into the roles of

the relaxins and cognate receptor during zebrafish embryogenesis and in the vertebrate evolution.

3.0 MATERIALS AND METHODS

3.1 Experimental model

I use as experimental model the zebrafish (*Danio rerio*). It is a small tropical fresh-water fish belonging to the family Cyprinidae of order Cypriniformes. Due to its small size and ease of culture, the zebrafish has become a favourite model organism for biologists studying embryonic development. The development of the zebrafish is very similar to the higher vertebrates embryogenesis, including humans. Moreover, during the first days of their lives, the embryos are transparent. The zebrafish model organism database ZFIN (http://zfin.org/) contains all the information about this experimental model to develop and support integrated zebrafish genetic, genomic and developmental information. The zebrafish embryonic development is very rapid: at the first 24 hours after fertilization (hpf), all major organs are formed and within 2 days the fish hatch and start looking for food, after 3/4 months zebrafish are sexually mature and can generate new offspring. In particular: there are some landmark stages:
1-cell (0-0.7 h): newly fertilized egg. The nonyolky blastodisc segregates towards the animal pole.
Cleavage (1-2.5 h): rapid divisions of the blastodisc that occur without cell growth.
Midblastula transition (3 h): division rate begins to slow and genes begin to be transcribed.
Epiboly (4-10 h): the blastodisc flattens into a blastoderm and spreads to cover the yolk. Gastrulation (5-10 h): the blastoderm develops two layers (outer ectoderm, inner mesendoderm) by involution. Segmentation (10-24 h): somite pairs form sequentially, the tail develops and primary organ rudiments begin to form.
Pharyngula (from 1 day): the body plan characteristic of all vertebrates is present and functionally differentiated cells characterizing the nervous, muscular, and circulatory systems. Hatching (from 3 days): embryonic development is complete.
Feeding (from 4 days): The swim bladder fills and the larva actively begins to seek prey (Kimmel, 1995).

3.2 Animals

Zebrafish were purchased from a local pet shop and housed in mixed-sex groups in static tanks (approximately 20 L each) with airlift-driven photoperiod 14h light/10h dark as described (Kimmel et al., 1995; Westerfield, 1995). All zebrafish were feeded twice a day with tetrafood and artemia. They were treated with specific protocol for euthanasia methods and anaesthetized with tricaine MS-222 (tricaine methanesulfonate) 0.16mg/mL in Embryo medium (Westerfield, 1995).

3.3 Database search and sequence analysis

To identify the zebrafish *rln* gene, we used the amino acid sequence of *Anguilla japonica Rln* (BAJ22076.1) for a tblastn search in *D. rerio* nucleotide National Center for Biotechnology Information (NCBI) database. Amino acid sequence comparison of *D. rerio* and various teleost *Rln*, and of *D. rerio Rln/Rln3* and human RLN/RLN3 was carried out by ClustalW alignment program (Larkin et al., 2007; Goujon et al., 2010). Instead, to obtain the exon and intron length and the exon-intron organization of zebrafish and human *rxfp1* gene, we used Sequence Viewer function of the National Center for Biotechnology Information (NCBI) web site (http://www.ncbi.nlm.nih.gov). The Map Viewer function of the same web site was used to identify neighborhood genes of *rxfp1* on the zebrafish and human chromosomes.

3.4 RNA extraction and clean up

Total RNA from embryos and adult tissues were isolated using the Trizol reagent (Invitrogen). RNA clean up was performed by using the Qiagen RNeasy Mini Kit as recommended by the manufacturer. Quantification of the samples was performed by nanodrop 2000c (Thermo Scientific). RNA quality analysis was carried out on electrophoretic gel agarose. For the preparation of the agarose gel, the electophoretic apparatus was treated with NaOH 0.2M for 20 min and washed with sterile double distilled water (ddH_2O).

3.5 cDNA synthesis.

First strand cDNA was synthesized from 3 µg of total RNA in a final volume of 20 µL by reverse transcriptase Superscript III as

recommended by the manufacturer (Invitrogen, Milan, Italy). In particular, both for cloning and expression pattern analysis, RNA from 2 to 72 hpf whole embryos and from different adult tissues was used. After cDNA synthesis, the volume was brought to 50 µL by adding sterile ddH_2O.

3.6 Polymerase chain reaction (PCR) and quantitative Real Time PCR (qPCR)

We performed PCR in 25 µL reaction volume containing 0.2 mmol/µL dNTPs, 10 pmol of each nucleotide, 2.5 µL buffer (10 mmol/µL Tris–HCl, 1.5 mmo/µL $MgCl_2$, 50 mmol/µL KCl, pH 8.3), 7% dimethylsulfoxide (DMSO), 1.5 U TAQ DNA polymerase (Sigma) and X µL of cDNA template. PCR was carried out in a GeneAmp PCR System 9700 (Applied Biosystems) and consisted of an initial step at 95 °C for 3 min, followed by 38/40 cycles at 95°C for 1 min, 54/58 °C (depending on the primers pairs) for 1 min, 72 °C for 1 min and a final cycle of extension at 72 °C for 10 min. In order to clone specific sequences we used 7µL of cDNA as a template and 40 cycles of amplification. To analyse the expression pattern of the relaxins and receptors transcripts, we used 4µL of cDNA and 38 cycles of amplification, whereas, 1 µL of cDNA and 36 cycles of amplification for the *rplp0* transcript.

To perform qPCR, we designed specific primer sets for each gene by using the Primer3 program (Untergasser et al., 2007 (http://www.bioinformatics.nl/cgibin/primer3plus/primer3plus.cgi). The primers, spanning an exon–exon boundary, amplify products of about 100 bp in length. Blast searches were used to ensure that primers were specific for each individual gene. The real-time PCR efficiency was calculated from the slope in the 7500 Software v.2.0.1 (Applied Biosystem). The relative quantification of gene expression was performed by real-time PCR using the SYBR Green JumpStart Taq ReadyMix (Sigma), in the Applied Biosystem 7500 Fast real-time PCR System. The following conditions were used: holding stage at 95 °C for 10 min, 40 cycles of 95 °C for 15 s and 60 °C for 1 min, followed by melt curve analysis to ensure that only a single PCR product was amplified. The specificity of real-time product amplification was also checked each time with high resolution

gel electrophoresis. Each 25 µL reaction contained 12.5 µL SYBR Green reagent ready mix 2X (Sigma), 0.25 µL ROX 100X (Sigma), 2.5 µL forward and reverse primer mix (4 mM) and 1 µL cDNA. To confirm accuracy and reproducibility of real-time PCR the intra-assay precision was determined in three repeats within each run. Control reactions (without template) were run for each sample in triplicate. ΔΔCt-Method was used for relative quantification. The relative gene expression levels were normalized to the *rplpo* transcript in the respective sample. The ΔCt was calculated by subtraction of the Ct value of the gene of interest from the Ct value of the reference gene (*rplpo*). ΔΔCt was calculated by subtracting the sample ΔCt to calibrator ΔCt. As a calibrator, we used the sample that showed the lowest level of transcript, (heart), 24 hpf for *rln* transcript and 0 hpf for *insl-5*a and *insl-5*b. The fold difference was calculated as ^{2}-ΔΔCt, as described in the "Guide to Performing Relative Quantitation of Gene Expression Using Real-Time Quantitative PCR" (Applied Biosystems). The PCR products obtained from different stages and tissues were electrophoresed on 1%-1.5%-2% (depending on the product length) agarose gel in Tris-Acetate-EDTA (TAE) 1X with EtBr 10 µg/mL.

Table 1: Primers for RT-PCR with relative accession number of genes:

gene	Accession number	Primers sequence
rln	JN215212	For 5′GAGTGTAGCTCTGTCTGTCT-3′ Rev 5-TCAGACTCAGCGCAGCTC- 3′ For qRT 5′-GCGGAGAGCGGACACA-3′ Rev qRT 5′-CAGGAGAACCGACTTCAGGA-3′
rxfp1	NM_001190934	For 5' TGTGAATGTTCCCAATTTCG 3' Rev 5' TTTGACCTTCTCGGGTCTTC 3'
rxfp3-1	NM_001128788	For 5' AGCGACGATTTTATCCAAGG 3' Rev 5' CACTTTGGAGCGCCTTTTAG 3' For 1 5' AACGCGATTTTCTCAACGAC 3' Rev1 5' CCGTTCTGTTTGGAATCTGG 3'
rxfp3-2a	XM_001346785	For 5' AACATCTCTGTAGCGCATG 3' Rev 5' CGCGGAGCAGAGGTATAC 3' For1 5' GCTCTCTGTCCTCTTCTTTGC 3' Rev1 5' CCCAAACTAGCCCACTTGAC 3'
rxfp3-2b	NM_001083879	For 5' CTCCGTTTACATCCTTTGAC 3'

		Rev1 5' TGCTTCGTCCTGTCAATC 3' For1 5' GCGTGGCAAGGTACTACTCC 3' Rev1 5' GCTGCTGCTCTGCGACG 3'
rxfp3-3a1	ENSDARG00000069028	For 5' CATTTAACACTATCGCAGAGAG 3' Rev 5' CAGTCCACTGTCCAATTTGG 3' For1 5' CCCTTCCAGAAAGAAGTCTGTG 3' Rev1 5' GTCGCCAGGATCCACAAC
rxfp3-3a2	ENSDARG00000062111	For 5' TCAACAACAGTTTGGTAGAATG 3' Rev 5' AACCCATTAATCACGGAAAG 3' For1 5' CAGAGGCTGTCAATGAGG 3' Rev1 5' TGACGGCGATGAGTATTACG 3'
rxfp3-3a3	ENSDARG00000069246	For 5' CTTCAACACGGGCTTTGC 3' Rev15'AAACAATACATCATCGTGTGAT 3' For1 5' GTGGGTGCTCGCTACAGTC 3' Rev1 5' AGACTTCTCTCCGACCACAC 3'
rxfp3-3b	ENSDARG00000059348	For 5' AGGATCGCACGCGGTATAAGC 3' Rev 5' GTTCAGGCAGCTGTTGGAGTG 3'
rln3a	NM_001037803.1	For 5' AAAGCACAGGTAGACCATCGG 3' Rev1 5' TGCAGCCCCATTTGCAGCAGG 3'
ff1b	NM_131794	For 5' ACGGTGATGGACTTCAGAGC 3' Rev 5' ATCGCCCACCTTTAGTTCCT 3'
Rxfp2-like	ENSDARG00000068731	For 5' TGGCCAGTTTATCTGTTAGAAGG 3' Rev 5' TGATGCCCAGAGAGATGAAA 3'
Rxfp2a	ENSDARG00000032820	For 5' AATACAGCAAACGCGCATC 3' Rev 5' TCTACTGAAGGCTCGGCTTG 3'
Rxfp2b	NM_200443.1	For 5' CAGGATTTTTAGGAACCCAGTG 3' REV 5'TCCACTGAAAGCCTGAATGG 3'
Insl5a	NM_001037669	For 5' GATCCAGAAGACCCGAGAGA 3' Rev 5' TGATTACTGCCTTCCACCAAC 3' For qRT5'TCAACTCTCTCCGAGATCCTCAAC3' RevqRT 5' GTGCGGCAGAGAGTTTATCC-3'
Insl5b	NM_001128556	For 5' GAAGACATTCTGAGGTCAG 3' Rev 5' CGACGTTTGAACATTTCTCAT 3' Rev qRT CCAAACTGAAGACCCCGTAA-3'
rplpo	NM_131580	For 5' CAAGGCCGTCGTGCTCA 3' Rev 5' CAGCGTGGCCTCGCTG 3' For qRT 5'CTGGAAAACAACCCAGCTCT-3' Rev qRT 5' CGGACCTCAGTCAGATCCTC-3′

3.7 Cloning in pGEM®-T Easy Vector

Amplicons were cloned into pGEM®-T Easy Vector (Promega) as recommended by instruction manual. The reaction have been optimized using a 3:1 molar ratio of the insert DNA to the vectors.

3.8 *RNA Probes for in situ hybridization experiments*

All solutions were prepared with DEPC water and RNase-free chemicals. RNA probes were obtained by in vitro transcription of inserted DNA into pGEM®-T Easy Vector, the linearized *rln* cDNA-containing plasmid, using DIG RNA Labeling Kit (Roche Diagnostics) as recommended by the manufacturer. The RNA riboprobe was precipitated by adding 5 µL of LiCl 4 M and 150 µL absolute ethanol and incubation at −20 °C over night. The pellet was washed with ice cold 70% ethanol and allowed to air-dry. The probe was resuspended in 50 µL of DEPC water.

3.9 Whole mount embryo in situ hybridization

The embryos were grown in embryo medium at 28.5 ºC until the desired developmental stage. After chorion removal, the embryos were fixed in 4% paraformaldehyde for two hours. When required, the pigmentation was removed by photobleaching. After dehydration with progressive passages in MeOH, the embryos were stored at -20 ºC.

For the *in situ* hybridization experiments, we used an antisense digoxigenin (DIG)-labeled RNA probe. The corresponding sense RNA probe was used as a control for the specificity of hybridization signals. Whole mount *in situ* hybridizations were carried out as reported in Thisse et al, (2004) with the following modifications: after the protease K digestion and fixing in paraformaldehyde, the embryos were incubated in triethanolamine (0.1 mmol/L pH 7.0) for 5 min and twice in triethanolamine-acetic anhydride solution for 5 min; the embryos were hybridized at 60 °C for 40 hr in the following hybridization mix: HM [50% formammide, 5X saline sodium citrate (SSC), 0.1% Tween 20, citric acid to pH 6.0, 5 mmol/L ethylenediaminetetraacetic acid (EDTA), 1X Denhardt's solution and Heparin 50 µg/mL, tRNA 500 µg/mL]; after hybridization, the following washes were performed: 15 min in 75% HM/25% 2X SSC at 60 °C, 15 min in 50% HM/50% 2X SSC at 60 °C, 15 min in 25% HM/75% 2X SSC at 60 °C, two washes of 10 min in 2X SSC at 65 °C, four washes of 10 min in 0.2X SSC at 65 °C; the incubation with anti-DIG antiserum was performed overnight at +4 °C in the following antibody solution: 100 mmol/L Tris–HCl pH 7.5, 150 mmol/L NaCl, 2% blocking reagent (Roche), 2 mg/mL BSA, 0.1%

Tween, 5% lamb serum. Finally, the digoxigenin-labeled cRNA probe was detected using anti-DIG-conjugated alkaline phosphatase activity and 4-nitroblue tetrazolium chloride/5-bromo-4-chloro-3-indolyl-phosphate (NBT/BCIP) (Roche) as substrate. For double *in situ* hybridization experiments, an *rln3a* fluoresceine-labeled RNA probe was used. The detection was performed by anti-FLUO-conjugated alkaline phosphatase activity and INT/BCIP (Roche) as described in Donizetti et al, (2009). *In situ* hybridization experiments were performed at least in triplicate for each embryonic developmental stage.
For transversal sections (3 μm) via ultramicrotome, the embryos were washed in PBT for 10 min (2 times) and were dehydrated by the following solutions: EtOH 25%/PBT 75%, EtOH 50%/PBT 50%, EtOH 75%/PBT 25%, EtOH 80%/PBT 20%, EtOH 95%/PBT 5%, EtOH 100%. After dehydration, the embryos were treated by 100% propylene oxide (4 times for 5 min), propylene oxide 75%/epon 25% (30 min), propylene oxide 50%/epon 50% (30 min), propylene oxide 25%/epon 75% (30 min), epon 100% (30 min), epon 100% (overnight at 70 °C).

Table 2: Proteinase K times for each zebrafish embryonic stage.

Embryonic stages	times for protease K
8 hpf	1’
16 hpf	5’
20 hpf	7’
24 hpf	10’
36 hpf	15’
40 hpf	17’
48 hpf	20’
72 hpf	25’
96 hpf	30'
120 hpf	35'

3.10 In situ hybridization on zebrafish adult tissues.

Danio rerio tissues were treated according to the following protocol: fix in Bouin 72h, wash in 70% EtOH 30 min, 4 times, washed in 80% EtOH 1h, dryed in 95% EtOH 30 min for 8 times, 100% EtOH 15 min for 4 times, Xylene 10 min for 4 times, paraffin embedding 42h. The slides were treated in xylene 10 min two washes, in 100% EtOH for 5 min, 95% EtOH, 80% EtOH, 70% EtOH, 50% EtOH EtOH, 30% EtOH 2 min each step in DEPC H_2O. The slides were incubated in Proteinase K 10 mg/ml in 20 mM Tris-HCl pH 7.2, 1 mM EDTA 20 min at RT or 10 min at 37 ºC. After, the slides were fixed in paraformaldehyde in 0.5 M NaCl, 0.1 M MOPS pH 7.5, 30 min RT, after they were washed in tris-glycine 5 min. Then, the slides were refixed in paraformaldehyde and treated with 10 mM triethanolamine in PBS 1X in DEPC and acetic anhydride. The tissues were washed in 2X SSC 2 min and in Tris-glycine 30 min at RT. The tissues were hybridized for 3 h at 50 ºC as follow: 40% formamide, SSC 5X, 1X Denhardt, Testis salm 100 µg/mL with the probe: 80 ng probe to slide. The hybridization solution is denatured at 95 ºC for 2 min, then kept on ice until hybridization at 50 ºC. The slides were washed in 2X SSC 20 min at RT, washed in 1X SSC and 20% Formamide at 60 ºC for 40 min and washed in 0.5 X SSC and 20% Formamide at 60 ºC 40 min. After, the slides were washed in NTE buffer 0.5 M NaCl, 10 mM Tris-HCl pH 7.0, 0,5 mM EDTA for 15 min at 37 ºC. The tissues were washed in NTE buffer + 10µg/ml RNase A, at 37 ºC 30 min and washed in NTE buffer at 37 ºC 15 min. The tissues were washed in 0.5X SSC and 20% Formamide for 30 min at 60 ºC and washed in 1X SSC for 30 min at RT. The slides were incubated with 100 mM Tris/HCl pH 7.5, 150 mM NaCl and Ab (diluted 1:2000 anti-digoxigenin Ab, and anti-fluorescein Ab 1:1000 Roche). For detection the slides were washed in TBS after in Tween 20 and 10 min Levamisole. The slides were washed with NMT detection buffer for 5 min at RT, incubated in NMT, NBT/BCIP (Roche). Wash slides in 1X PBS and 1 mM EDTA, 30 minutes. the slides were dehydrated with 50% EtOH, 70% EtOH, 80% EtOH, 90% EtOH, 100% EtOH, after washes in xylene. Close the slide through clearing agents to a point at which a permanent resinous substance beneath the glass coverslip, or a plastic film, can be placed over the section.

4.0 RESULTS

4.1 RELAXIN LIGANDS

4.1a Relaxin

We started with searching for the *rln* coding region in *D. rerio* genome. We used the amino acid sequence of *A. japonica Rln* (BAJ22076.1) as a bait for a tblastn search in the *D. rerio* nucleotide collection database of the NCBI website. We found a genomic region containing the putative *rln* coding region that we used to design a couple of primers in the 5′UTR and 3′UTR of zebrafish *rln* transcript. For the RT-PCR amplification, we used the corresponding cDNA of RNA extracted from embryos at 48 hpf (hours post fertilization) and adult brain. The resulting amplicon (575 bp) was cloned and sequenced (AC: JN215212) to confirm the specificity of the amplification reaction. The corresponding translated amino acid sequence was used to retrieve orthologue Rln sequence in other fish species by a tBLASTn search in the NCBI database (*http://blast.ncbi.nlm.nih.gov/Blast.cgi*). In Figure 5A, it is shown the overall amino acid sequence alignment of zebrafish Rln with some orthologue sequences found in different fish species. As expected, the B and A domains, which should be retained in the mature molecule, showed higher amino acid sequence conservation than the C domain. In the Figure 5B, we reported the B and A domains alignment of zebrafish Rln, Rln3a and Rln3b, and human RLN1/2 and RLN3 proteins. The B domain of zebrafish Rln sequence showed greater similarity to the corresponding domain of zebrafish Rln3a/b (80%) and human RLN3 (76%) than to the B domain of human RLN1/2 (44%). Differently, the zebrafish Rln A domain showed relatively low amino acid sequence similarity when compared to the corresponding sequence of the other aligned proteins (≤ 45%) (Figure. 5B). The greater diversity of the A domain respect to B domain may reflect different binding specificity for the relaxin receptors compared to Rln3 peptides. The identification of zebrafish *rln* orthologue gene was further supported by the exon-intron organization and the syntenic analysis. In particular, the analysis of genomic sequence showed that *rln* gene is split into two exons by an intron sequence of 2845 base pairs length (Figure. 5C). In line with data reported by Good-Avila et

al. (2009), the *rln* gene was found on the chromosome 21 between *Jak2* and *C9orf46* genes (Figure. 5C), showing conserved syntenic organization compared to other teleost orthologues.

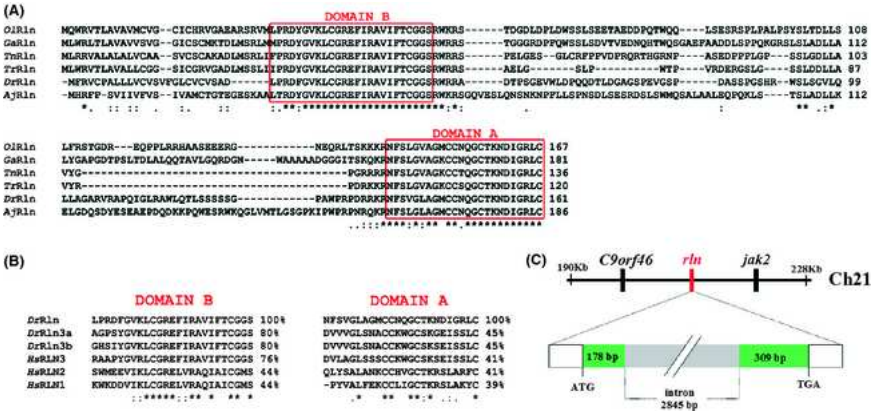

Figure. 5. **Comparative analysis of Rln amino acid sequence and gene structure.** Amino acid sequence alignment of the zebrafish *rln* with the ortologue sequence of other teleost species (in panel A). The number on the right indicates the amino acid sequence length. Amino acid sequence alignment of B and A domain of zebrafish Rln, Rln3a/b and human RLN3 and RLN1/2 (in panel B). Genomic organization and syntenic analysis of the zebrafish *rln* gene (in panel C). Identical amino acids are indicated by asterisks, conservative substitutions are shown by colons and semiconservative substitutions by dots. Gaps in the sequence are represented by dashes. The alignments in A and B were carried out by ClustalW software with default parameters. OlRln, *Oryzias latipes* Relaxin (NP_001098341.1); GaRln, *Gasterosteus aculeatus* Relaxin (ENSGACG00000017364); TnRln, *Tetraodon nigroviridis* Relaxin (ACA13590.1); TrRln, *Takifugu rubripes* Relaxin (NP_001092113.1); DrRln, *Danio rerio* Relaxin (JN215212); DrRln3a, *D. rerio* Relaxin3a (NP_001032892); DrRln3b, *D. rerio* Relaxin3b (NP_001108535); AjRln, *Anguilla japonica* Relaxin (AB576118); HsRLN1, Homo sapiens Relaxin1 (NP_008842); HsRLN2, Homo sapiens Relaxin2 (NP_604390); HsRLN3, H. sapiens

Relaxin3 (AAQ88548). The percentage value indicates the amino acid sequence similarity.

To evaluate the *rln* transcript level during embryogenesis and in the adult tissues, we carried out RT-qPCR experiments. During embryogenesis, the *rln* transcript was revealed in all the analysed stages, including cleavage stage (2 hpf), suggesting a maternal origin of the transcript (Figure. 6A). The transcript level decreased from cleavage (2 hpf) to the sphere stage (4 hpf), whereas it newly increased at the blastula stage (8 hpf) (Figure. 6A). Subsequently, from the low level detected during somitogenesis (16 hpf), a progressive increase in the transcript amount was revealed until the larval stage (72 hpf) (Figure. 6A). In the adult, the *rln* transcript was detected in all the analysed tissues; in particular, a relatively higher transcript amount was evidenced in the brain than in the other tissues (Figure. 6B).

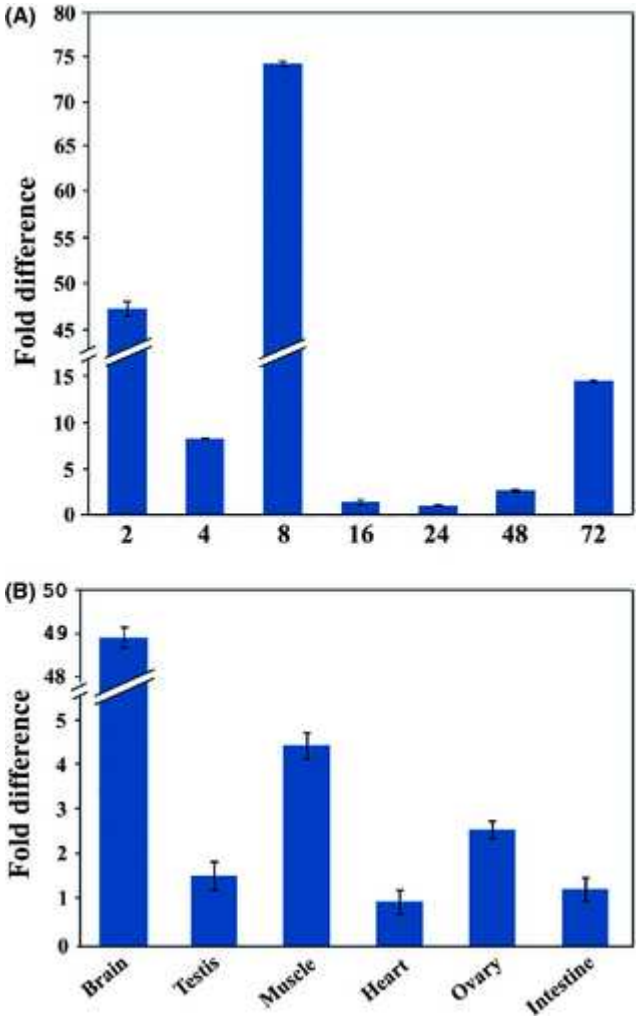

Figure. 6. **Expression pattern of the *rln* gene by RT-qPCR.** Fold difference of *relaxin* gene expression at indicated stages as hours postfertilization (hpf) (A). Fold difference of *relaxin* gene expression in various tissues of adult zebrafish (B). *Relaxin* expression levels were normalized against *rplpo* transcript. Black bars represent the standard deviation.

Moreover, in order to identify embryonic territories of *rln* gene expression, we carried out whole mount *in situ* hybridization experiments on zebrafish embryos at different developmental stages. In particular, to detect *rln* mRNA, we used a DIG-labeled antisense riboprobe, and, to control the specificity of the hybridization signals, we used the corresponding DIG-labeled sense riboprobe. Likely as a consequence of low transcript amount, the appearance of specific hybridization signals required relatively long staining reaction time. That determined the appearance of aspecific background staining. In light of that, we only took into account hybridization signals that were clearly evidenced by comparison between sense (Figure. 7A, C, F, H, J, L, P) and antisense riboprobe experiments (Figure. 7B, D, E, G, I, K, M, Q, R, S, T). From fertilized eggs to somitogenesis, we revealed broadly distributed hybridization signal (data not shown). Starting at pharyngula stage (24 hpf), we detected restricted *rln*-expressing cells in the olfactory placodes (Figure. 7B). At late pharyngula stage (48 hpf) *rln* transcript continued to be detected in the olfactory placodes (Figure. 7G). Later, the transcript was still revealed in the same cell groups at the larval stage (72 hpf) (Figure. 7I), whereas it was no longer detected in that region at the post-embryonic analysed stages (data not shown). At the 24 hpf embryonic stage, *rln* gene expression was also revealed in the posterior branchial arch region (Figure. 7D). This hybridization signal was evident until 30 hpf, when new *rln*-expression territory was revealed close to the otic vescicle (Figure. 7E). At larval and post-embryonic stages, new expression territories were detected. In particular, the gene expression was revealed in restricted brain regions, such as preoptic area (Figure. 7K) and, posteriorly, in some scattered hindbrain cells (blue arrowheads) and in a bilateral cell cluster in the pons region, as shown by dorsal view (Figure. 7M). The same hybridization signals were also revealed at 96 hpf and 120 hpf (data not shown). The bilateral cell cluster in the pons region appeared similar to that previously described by our group for the *rln3*a expression pattern analysis (Donizetti et al., 2008; 2009). By double *in situ* hybridization experiments, we showed colocalization of *rln* and *rln3*a transcripts. In this regard, we used antisense *rln* DIG-labeled and *rln3*a fluorescein-labeled cRNA probe. The *rln3*a riboprobe marked the anterior cell cluster in the central midbrain tegmentum (orange arrow), that we hypothesized as a homologous region of mammalian periaqueductal gray (Donizetti et

al. 2008; 2009), whereas *rln* riboprobe marked scattered cells in the hindbrain region (blue arrowheads) (Figure. 7N). In addition, both riboprobes co-localized in the cell cluster of the pons region (blue/orange arrowhead in Figure. 7N), as better evidenced by the magnification (Figure. 7O). At 96 hpf, a new signal was revealed around the anterior commissure (Figure. 7S). Starting at larval stage (72 hpf), the *rln* transcript was also detected in the pancreatic region, as shown in a lateral view of the embryo (Figure. 7Q). Later, *rln* gene expression persisted in the pancreatic region at 96 hpf (data not shown) and 120 hpf, when *rln* transcript-positive cells appeared circularly distributed (Figure. 7T). An additional signal was also revealed in thyroid gland at 96 hpf (Figure. 7R) and 120 hpf (data not shown).

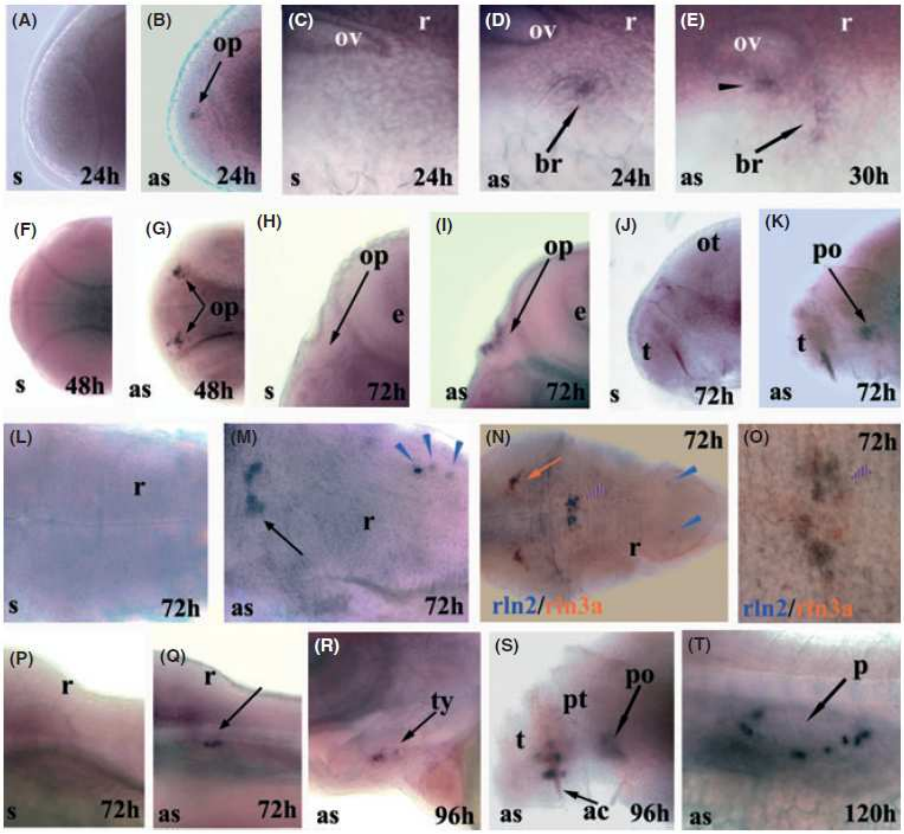

Figure. 7. **Localization of the *rln* transcript by whole mount *in situ* hybridization at indicated stages of zebrafish embryogenesis.** Control experiments with *rln* sense riboprobe (A, C, F, H, J, L, P). *In situ* hybridization experiments with *rln* antisense riboprobe (B, D, E, G, I, K, M, Q, R, S, T). Double *in situ* hybridization experiments with *rln* and *rln3a* antisense riboprobes (N, O). Lateral view of embryo at early pharyngula stage, head region (A, B). Lateral view of embryo at early pharyngula stage, particular of pharyngeal arches region (C–E). Ventral view of embryo at late pharyngula stage, head region (F, G); Magnification of the olfactory placode region at larval stage (H, I). Lateral (J, K) and dorsal view (L, M, N, O) of brain embryo at larval stage; (N) double *in situ* hybridization for *rln* transcript (blue signal) and *rln3a* transcript (orange signal) at larval stage; magnification of rhombencephalic region where *rln* and *rln3a* transcripts colocalized

(O). Particular of anterior trunk region (P, Q). Lateral view of head region of post-embryonic zebrafish (R). Lateral view of anterior brain region of post-embryonic zebrafish (S). Magnification of pancreatic region of post-embryonic zebrafish (T). Black arrowhead indicates *rln*-expressing cells near otic vescicles; blue arrows indicate rhombencephalic cells. Blue/orange arrowhead indicates colocalization of *rln* and *rln3a* transcripts. ac, anterior commissure; br, branchial region; e, eye; op, olfactory placode; ov, otic vescicle; p, pancreas region; po, preoptic region; pt, prethalamus; r, rhombencephalon; t, telencephalon; ty, thyroid.

4.1b INSL-5a and INSL-5b

Furthermore, we analyzed the two zebrafish *insl-5* paralogues genes, *insl-5*a and *insl-5*b. To have information on the *insl-5*a and *insl5*b transcript level during embryogenesis, we carried out RT-qPCR experiments on total RNA extracted at various developmental stages. The *insl-5*a and *insl-5*b transcripts are present in all the embryonic stages, including cleavage stage (2 hpf), suggesting a maternal origin (Figure. 8A). The *insl-5*a transcript amount increased at sphere (4 hpf) stage, and resulted at similar level at blastula (8 hpf) and the somitogenesis stage (16 hpf). Subsequently, the transcript level decreased from early pharyngula (24 hpf) to larval stage (72 hpf). *insl-5*b showed a different expression pattern compared to *insl-5*a. We observed the highest transcript level at cleavage stage (2 hpf) (Figure. 8). The RNA amount decreased until blastula stage (8 hpf) to re-increase at somitogenesis stage (16 hpf). At early and late pharyngula stage (24 hpf and 48 hpf), we observed a relatively low transcript level, while at larval stage (72 hpf), a new increase was revealed (Figure. 8).

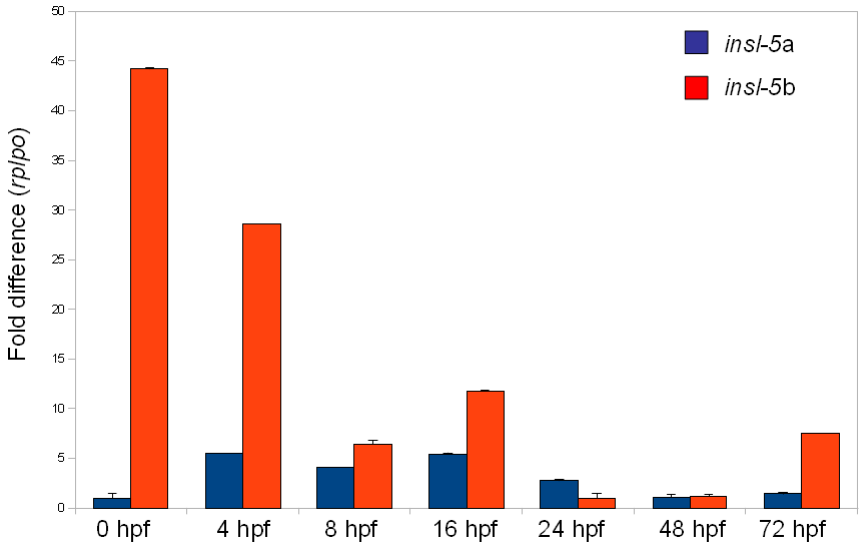

Figure. 8. **Expression pattern of the paralog gene *insl-5*a and *insl-5*b RT-qPCR.** Fold difference of *insl-5*a and *insl-5*b gene expression at indicated stages as hours post-fertilization (hpf). The expression levels were normalized against *rplpo* transcript. Black bars represent the standard deviation.

To localize the expression territories, we carried out *in situ* hybridization on *insl-5*a and *insl-5*b paralogues genes at different zebrafish development stages. We observed a restricted hybridization signal for *insl-5*a starting from 72 hpf (larval stage) until 96 hpf. In particular, gene expression was revealed in intestinal cells and pancreatic region (Figure. 9). On the contrary, *insl-5*b showed a very faint hybridization signal and only at 96 hpf, we were able to detect a specific and restricted signal in intestinal cells (Figure. 9). To better characterize the intestinal cell types where the two paralogue genes are expressed, we performed *in situ* hybridization experiments on sections of adult zebrafish intestine tissue (Figure. 10 and 11). As a control, we carried out hybridization experiments using RNA sense probe (Figure. 10A and 11A). The two genes showed expression in two different cell types. In particular, *insl-5*a is expressed in the goblet

cells (Figure. 10B and a magnification in D), while *insl5*b is expressed in the enteroendocrine cells (that are specialized endocrine cells of the gastrointestinal tract) (Figure. 10B and a magnification in D).

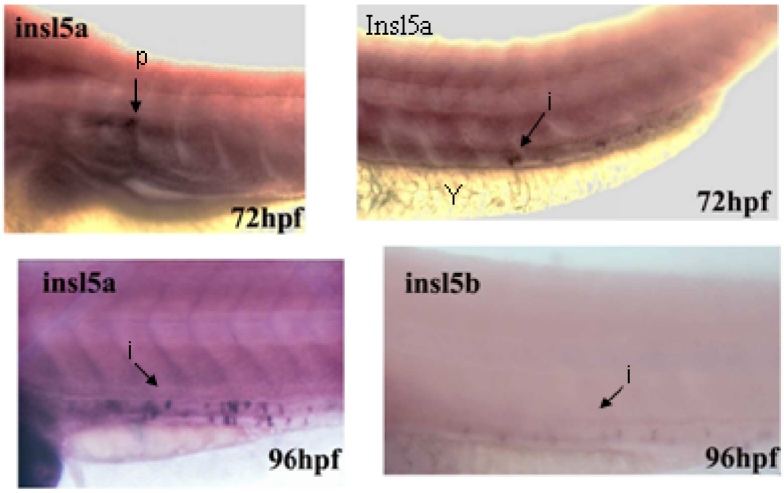

Figure. 9. **Whole mount *in situ* hybridization for *insl-5*a and *insl-5*b paralogues genes at indicated zebrafish developmental stage.** i: intestine; y: yolk; p: pancreatic region.

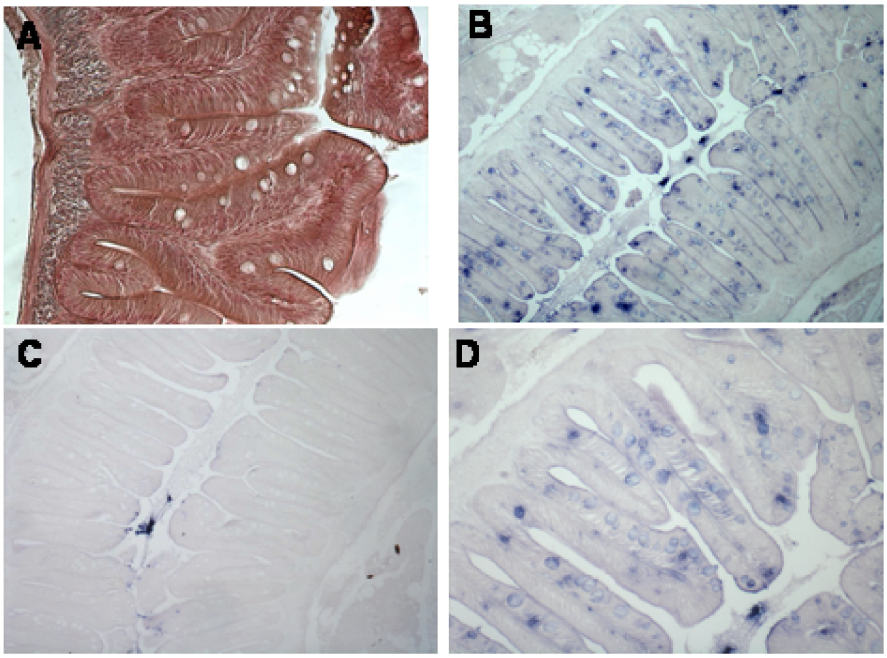

Figure. 10. **Histological intestine cross section of adult zebrafish intestine tissue.** Cross section coloured with counterstained with haematoxylin and eosin (A). *in situ* hybridization with antisense *insl-5a* probe (B) and relative magnification (D). *in situ* hybridization with *insl-5a* sense probe (C).

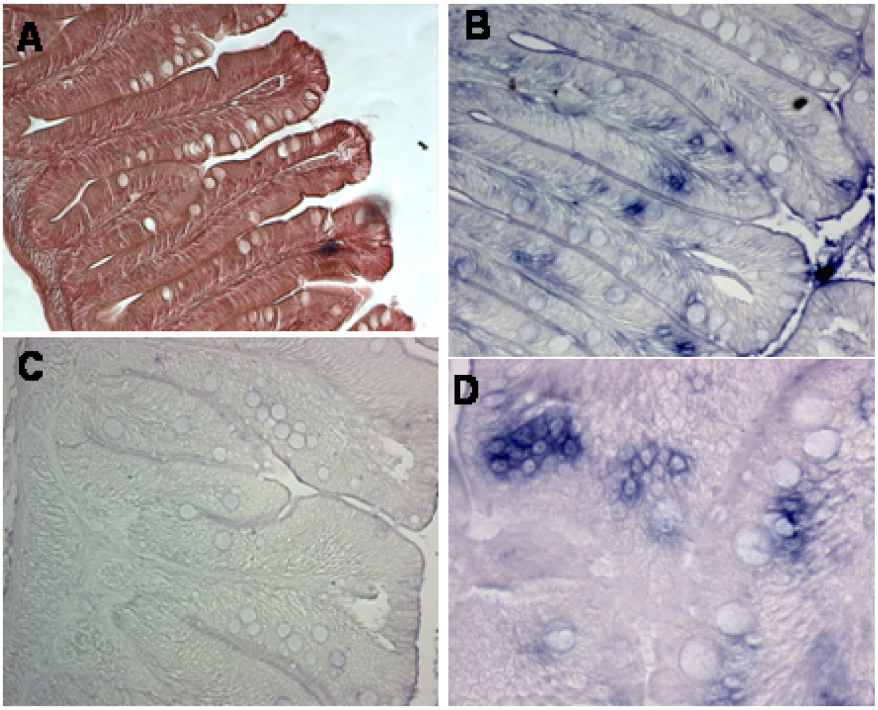

Figure. 11. Histological intestine cross section of adult zebrafish intestine tissue. Cross section coloured with counterstained with haematoxylin and eosin (A). *in situ* hybridization with antisense *insl-5*b probe (B) and relative magnification (D). *in situ* hybridization with *insl-5*b sense probe (C).

4.2 *RELAXIN RECEPTORS*

4.2a rxfp1

In order to identify the zebrafish homologue of the human RXFP1, we used the amino acid sequence of the human receptor (NP_067647) as a bait to perform a tBLASTn search in the NCBI nucleotide database (*http://www.ncbi.nlm.nih.org*). By this approach, we identified a predicted *Danio rerio* mRNA sequence reported in the database as ‘‘similar to relaxin/insulin-like family peptide receptor 1’’ (XM_688573). Based on the nucleotide sequence, we designed a

series of primers to amplify (by RT–PCR experiments) and clone the full-length cDNA coding region of the zebrafish *Rxfp1* receptor. The PCR products were cloned and sequenced to confirm the full-length cDNA coding region sequence (HM135955). The alignment of deduced zebrafish and human RXFP1 protein showed 76% amino acid sequence similarity (Figure. 12). All of the characterizing extracellular domains of the RXFP1 receptor are present in the zebrafish sequence. As displayed in Figure 12, the high degree of conservation is also reflected in potential N-glycosylation sites, in potential phosphorylation sites and in key amino acid residues important for receptor activation and interaction with RLN2 (Bullesbach & Schwabe 2005; Halls et al., 2007; Hopkins et al., 2007; Yan et al., 2008).

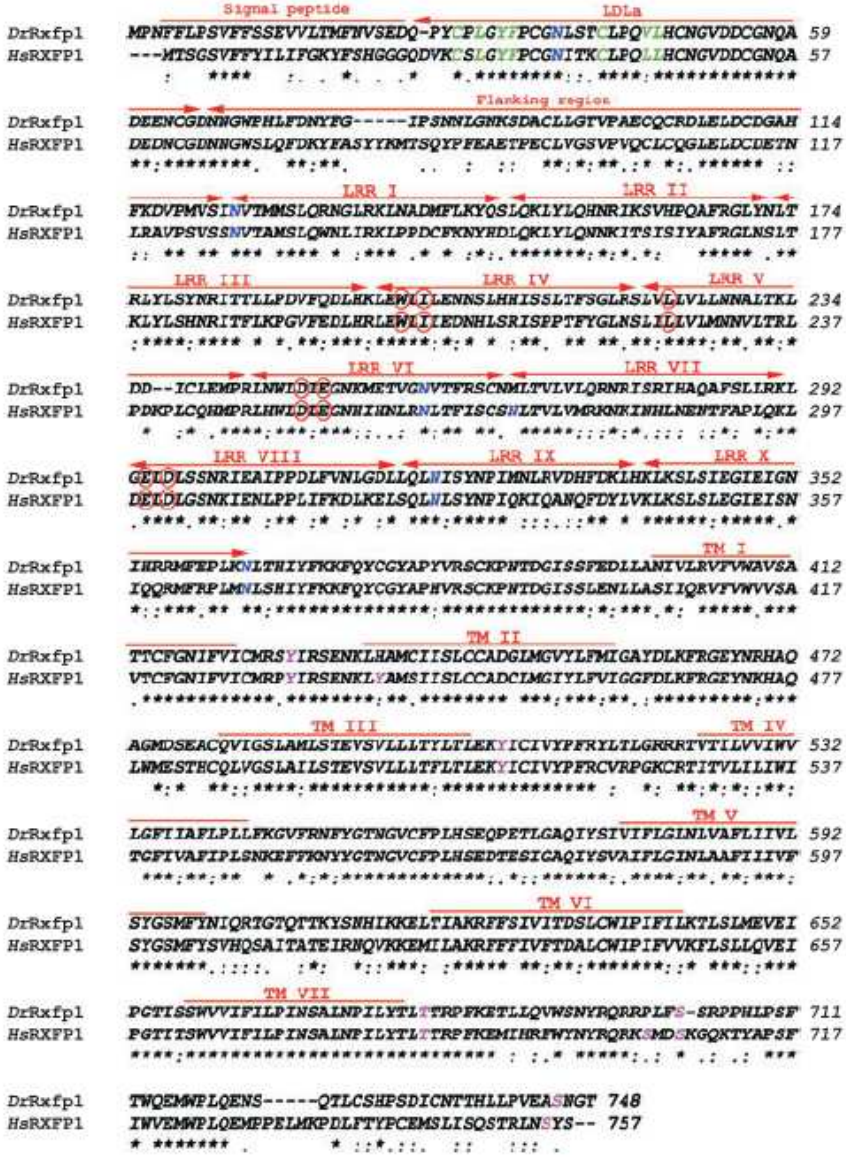

Figure. 12. Amino acid alignment of the human RXFP1 (HsRXFP1; NP_067647) and zebrafish *Rxfp1* (*DrRxfp1*; HM135955) proteins using ClustalW. The amino acid residues important for receptor activation are in green. The potential N-

glycosilation sites are indicated in blue. The putative phosphorylation sites are indicated in pink. The circles indicate the residues of the relaxin binding site in the leucine-repeats of the receptor. Identical amino acids are indicated by asterisks (*), conservative substitutions are shown by colons (:), and semiconservative substitutions by full points (.). Gaps in the sequence are represented by dashes. LDLa is the low density lipoprotein module; LRR indicates the leucin rich region; TM is the transmembrane region.

In addition, we compared the genomic sequences of the zebrafish and human RXFP1 genes. The comparison of the gene order in the neighborhood of the *rxfp1* in the zebrafish and human genome supported the idea that the identified zebrafish sequence is the homologue of the human RXFP1 receptor (Figure. 13b). The human RXFP1 gene is made up of 18 exons, where the first and second exons are separated by 50.6 kb. The zebrafish *rxfp1* gene is organized in 17 exons and, similarly to the human gene, the first exon is far from the second, being separated by 58.2 kb (Figure. 13a). The first exon of the zebrafish gene contains the coding region for both the signal peptide and LDLa module, whereas in the human genome the sequences for the two domains are split into two exons (Figure. 13a). The other exons of the human and zebrafish gene are highly conserved and encode for the same amino acid region (Figure. 13a).

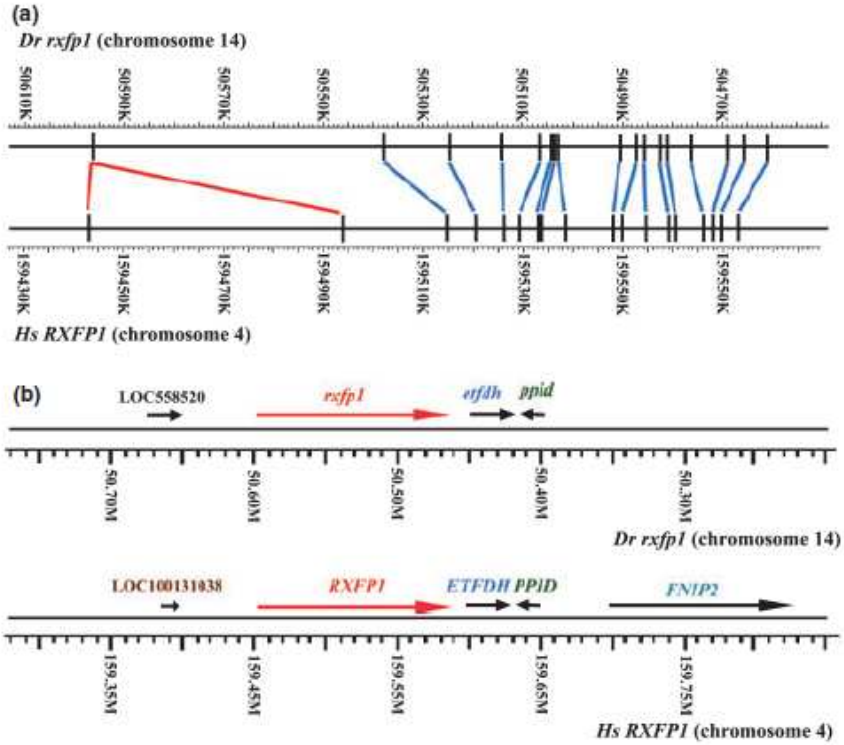

Figure. 13. **Schematic representation of the human RXFP1 and zebrafish *rxfp1*.** Exon/intron organization of the human RXFP1 and zebrafish *rxfp1* on the corresponding chromosomal region (a). The red lines indicate the difference in the first zebrafish *rxfp1* exon, which is split into two exons in the homologue human gene. The blue lines indicate the correspondence of the remaining exons in the two genes. Analysis of the neighborhood of the *rxfp1* gene in the zebrafish and in the human genome (b). The homologue genes are indicated with the same colours.

To look into the temporal expression pattern of the zebrafish *rxfp1* gene during embryogenesis, we carried out RT–PCR experiments on total RNA from different developmental stages. As shown in Figure 14a, the *rxfp1* transcript is present in all analysed stages with higher level at the blastula (4 hpf) and late pharyngula stages (48 hpf) (Figure. 14). The same RT–PCR analysis was carried out for the adult

organism, by using RNA extracted from different zebrafish tissues (Figure. 14b). Results of PCR amplification showed that the gene is broadly expressed, being actively transcribed in all the analysed tissues.

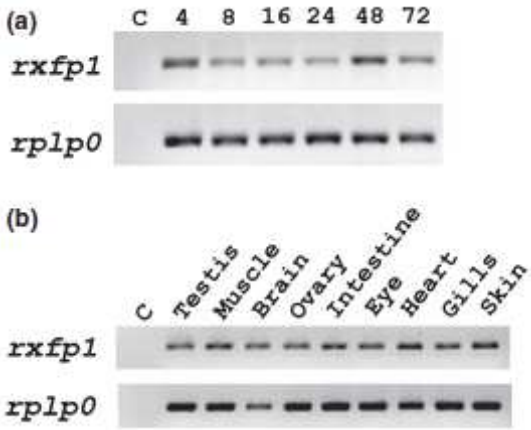

Figure. 14. **Temporal expression pattern of zebrafish *rxfp1* by RT-PCR experiments.** Analysis of *rxfp1* gene at different embryonic stages, indicated on top as hours post fertilization (a). Analysis of *rxfp1* gene expression in the adult zebrafish tissues (b). The control PCR reaction without cDNA template are indicated as C in (a) and (b). Amplification of *rplp0* cDNA fragment was a control of RT–PCR sensitivity in the assays.

We carried out whole mount *in situ* hybridization experiments, in order to analyse the embryonic territories of *rxfp1* gene expression. During the early developmental stages (4 hpf), the transcript appeared widely distributed in embryos (Figure. 15a), whereas during somitogenesis (16 hpf) the expression was restricted in the brain with a strongest hybridization signal in the diencephalic region (Figure. 15b, c). Starting from the pharyngula stage (24 hpf), the expression was evidenced in the epiphysis and in the branchial arch region, as

clearly shown by a lateral view of the embryo (Figure. 15d). A dorsal view of the head showed that the *rxfp1* transcript was also present in the diencephalic region and in the terminal nerve (Figure. 15e) as better shown in the magnification (Figure. 15f). At the late pharyngula stage (48 hpf), the *rxfp1* gene expression was still detected in the terminal nerve and in the epiphysis but not in the first branchial arch (Figure. 15g). In addition, a new expression territory was apparent in the postoptic region and in the hypothalamic region (Figure. 15g). A ventral view of the embryo highlighted the signal in the terminal nerve between the olfactory bulb and olfactory placode, and in two distinct cell groups in the postoptic region and, more caudally, in the ventral hypothalamic region (Figure. 15h). At this stage, other new *rxfp1*-expressing cells were detectable in the rhombencephalic region (Figure. 15i). At larval stage (72 hpf), the *rxfp1* expression persisted in the terminal nerve (Figure. 15j, k). The lateral and dorsal view of the brain clearly showed *rxfp1*-expressing cells in the epiphysis (better shown in the inset of Figure 15j), in the postoptic region, in the posterior tuberculum, in the hypothalamus, in the optic tectum, tegmentum/pons region and medulla region (Figure. 15j, l, m).

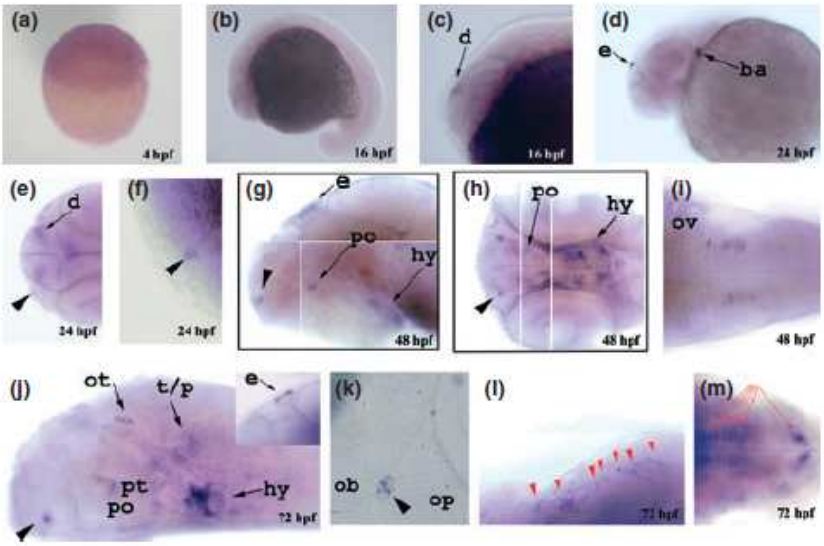

Figure. 15. ***In situ* localization of *rxfp1* transcript.** Embryo at blastula stage (a). Embryo at somitogenesis stage (b, c). Embryo at early pharyngula stage (d–f). Embryo at late pharyngula stage (g–i). Embryo at larval stage (j–m). The black arrowhead indicates the terminal nerve. The red arrowheads indicate cells in the optic tectum. The red arrows indicate cells in the rombencephalic region. ba, branchial arch; d, diencephalic region; e, epiphysis; hy, hypothalamic region; ob, olfactory bulb; op, olfactory placode; ot, optic tectum; ov, otic vescicle; po, preoptic region; pt, posterior tuberculum; *t*/p, tegmentum/pons region.

4.2b rxfp2

To analyze the temporal expression pattern of *rxfp2* paralogue genes during embryo development, we carried out RT–PCR experiments. We observed that only one of the three *rxfp2* paralogue genes, *rxfp2-like*, was expressed during zebrafish development. In particular, we detected the transcript at late pharyngula and larval stage (Figure. 16).

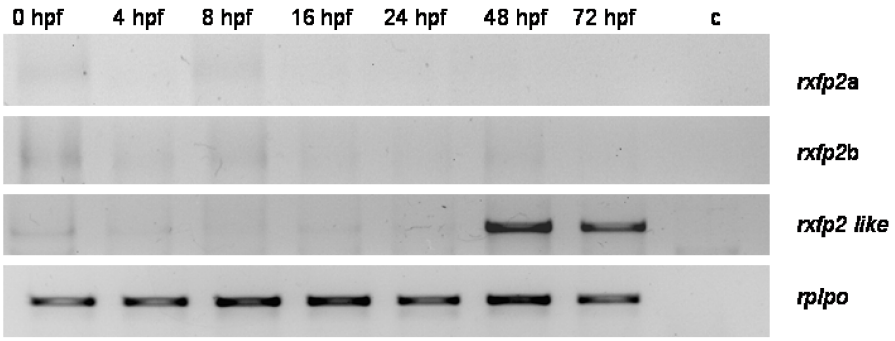

Figure. 16. Temporal expression pattern of zebrafish *rxfp2* paralogue genes by RT–PCR experiments at different embryonic stages indicated on top as hours post fertilization. Amplification of *rplp0* cDNA was used as a control of RT–PCR sensitivity in the assay. A negative control lacking cDNA template generated no PCR products (c).

Embryonic expression territories of *rxfp2-like* were analyzed by whole mount *in situ* hybridization experiments. We revealed hybridization signals only starting from 48 hpf, in accordance to RT-PCR data. The transcript was localized in the epiphysis as showed in Figure. 17 A, B, C. At late larval stage (96 hpf), we observed a new expression territory in the rhomboencephalic region, habenula and preoptic area.

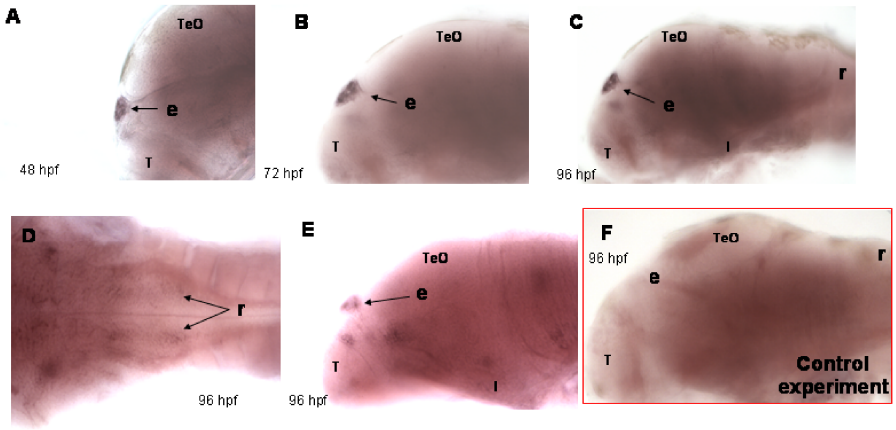

Figure. 17. Whole mount *in situ* hybridization of *rxfp2-like* gene. Lateral view of embryo at late pharyngula stage (A). Lateral view of embryo at early larval stage (B). Lateral view (C; E) and dorsal view of embryo at late larval stage (D). Lateral view of embryo at late larval stage as a control using sense riboprobe (F). e: epiphysis, i: Hypothalamus, r: rhomboencephalon, TeO: optic tectum, T: telencephalon.

4.2c rxfp3

Seven *rxfp3* genes have been reported for zebrafish genome. We investigated their temporal expression pattern during embryogenesis by means of RT-PCR analysis. No amplification products were obtained for *rxfp3-3a*2 and *rxfp3-3a*3 gene in all the analyzed embryonic stages (Figure. 18). The *rxfp3-3a*1 and *rxfp2-2*b amplicons were only revealed at larval stage, whereas the amplification product for the *rxfp3-1* gene was revealed from somitogenesis to larval stages (Figure. 18). Differently, the PCR amplification reaction for the *rxfp3-2*a and *rxfp3-3b* gene showed that the transcript was present in all the analyzed stages from 0 hpf to 72 hpf (Figure. 18).

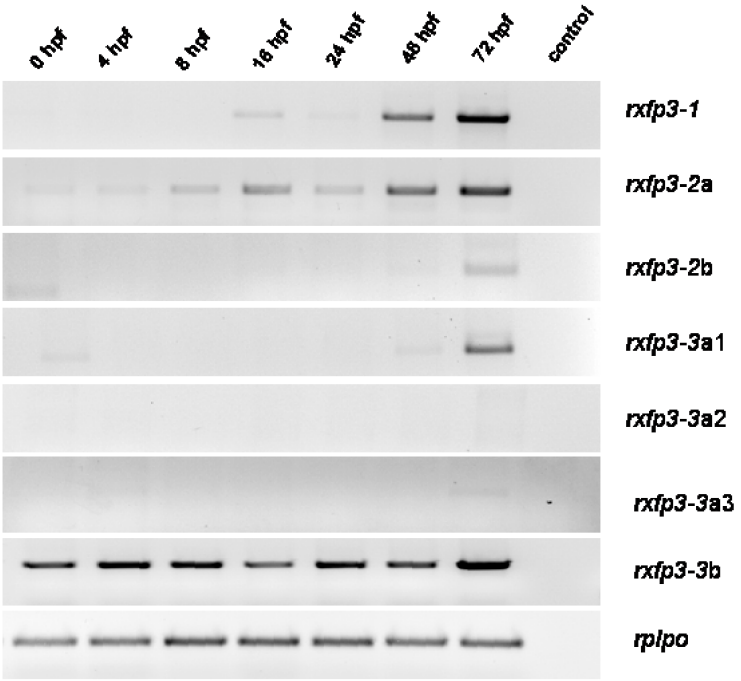

Figure. 18. Temporal expression pattern of zebrafish *rxfp3* homologues on total DNase-treated RNA by RT–PCR experiments at different embryonic stages (indicated on top as hours post fertilization). Amplification of *rplp0* cDNA was used as a reference gene. We performed negative control (experiments lacking cDNA template indicated as "control" in the panel) and on all RNA samples without retrotranscription (data not shown).

Embryonic localization of gene expression for *rxfp3* homologue genes has been characterized by whole mount *in situ* hybridization experiments on zebrafish embryos. By means of such technical approach, we confirmed that no transcript were present for *rxfp3-3a*2 and *rxfp3-3a*3 gene during embryogenesis (data not shown), as previously evidenced by RT-PCR experiments (Figure. 18). For what concerns the *rxfp3-3a*1 transcript, likely as a consequence of low

transcript amount, we were unable to obtain specific hybridization signal.

For *rxfp3-1* gene, at 24 and 48 hpf, the expression was clearly evidenced in a cell group in the middle/ventral region of the zebrafish trunk (Figure. 19). The dorsal view of the embryo showed that the cell cluster was located asymmetrically to the right of the notochord, in a position compatible with interrenal gland (Figure. 19). Moreover, at larval stage, we observed that the gene expression is localized in the rhombencephalic region (Figure. 19D, E).

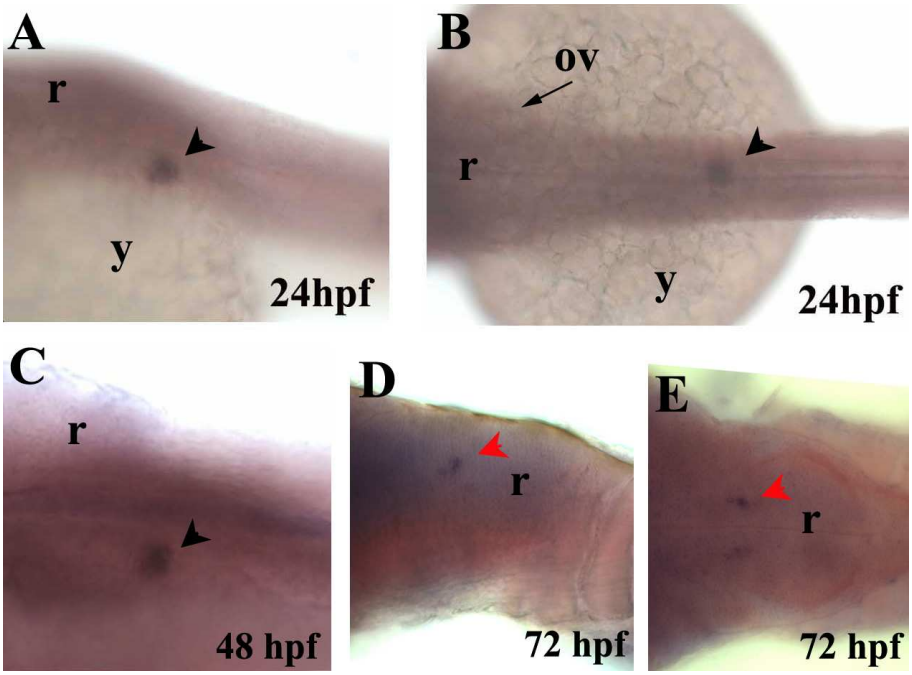

Figure. 19. **Whole mount *in situ* hybridization experiments for *rxfp3*-1 transcript.** Lateral view (A), dorsal view of embryo at pharyngula stage (B). Embryo at 48 hpf (C). Lateral view of embryo

(D) and dorsal view of embryo at larval stage (E). Black arrowhead indicates interrenal gland, red arrowhead indicates rhomboencephalon nuclei, Black arrow indicates otic vescicle. OV: otic vescicle, r: rhomboencephalon, y: yolk.

Concerning *rxfp3-2*a, we essentially found that the gene was mainly expressed in the developing brain, and, in addition, in the eyes and thymus. At somitogenesis stage (16 hpf), the *rxfp3-2*a transcript was revealed in the diencephalic region, as evidenced by a lateral view of the embryo (Figure. 20A). At the onset of pharyngula stage (24 hpf), *rxfp3-2*a gene expression persisted in the diencephalon region and a new transcript site was present in the ventral retina of the developing eye (Figure. 20B, C) and in the rhombencephalic region (Figure. 20D). At late pharyngula stage (48 hpf), the expression of *rxfp3-2*a gene was revealed in the ganglion cell layer of the retina (Figure. 20E). At this stage, the expression pattern showed a wide distribution throughout different developing brain areas. In particular, the transcript was detected in the epiphysis, diencephalon, optic tectum and rhombencephalic region (Figure. 20F). The transcript was also evidenced in the telencephalic region (Figure. 20F). Moreover, the *rxfp3-2*a expression was revealed in extraneural territories, in particular, the hybridization signal marked bilateral cell groups in the pharyngeal arch region corresponding to the thymus (Figure. 20F). We also analysed the *rxfp3-2*a gene expression at 72 and 96 hpf, essentially revealing similar expression pattern at both stages. In particular, *rxfp3-2*a expression persisted in the ganglion cell layer and in the thymus as well as in different cell clusters widely distributed in the brain (Figure. 20G). To better characterize the topographical distribution of the *rxfp-2*a transcript, we carried out serial transverse sections of the hybridized zebrafish larvae. Sections led us to reveal many cell clusters distributed in various regions of the larval brain, and, in addition in the ganglion cell layer and thymus (Figure. 21). In the forebrain, the expression of *rxfp3-2*a was evidenced in the pallium (Figure. 21a). In addition, in the transverse section, the transcript was also evident in a restricted cell cluster, which could represent either the telencephalic migrated area or the migrated entopeduncular complex (Figure. 21a). A staining was revealed in the epyphisis and

more laterally in a cell cluster located in the habenula (Figure. 21b). Different positive cell clusters were also present in the thalamic region and optic tectum, as evidenced by several transverse sections (Figure. 21b-k). The *rxfp3-2*a transcript were revealed in migrated pretectal area and in migrated posterior tuberculum area (Figure. 21C, h). Sections also revealed staining in cell groups which could represent, nuclei of various cranial nerve, as oculomotor, trigeminal, abducens, vagus and spinal motor nuclei (Figure. 21k, q-t). Finally, the expression was detected in cell clusters belonging to the region of nucleus of medial longitudinal fascicle, superior raphè, and in cell rows in the medulla oblongata (Figure. 21i, m-p, v-z). The analysis of *rxfp3*-2b transcript at larval stages (72 and 96 hpf) makes not possible the identification of specific signal, due to a faint hybridization signal with high interfering background (data not shown). This was in agreement with the transcript level revealed by RT-PCR experiments, which showed that the *rxfp3-2*b transcript was undetectable throughout the embryonic development and was revealed only starting at larval stages at a very low level in comparison to *rxfp3-2*a.

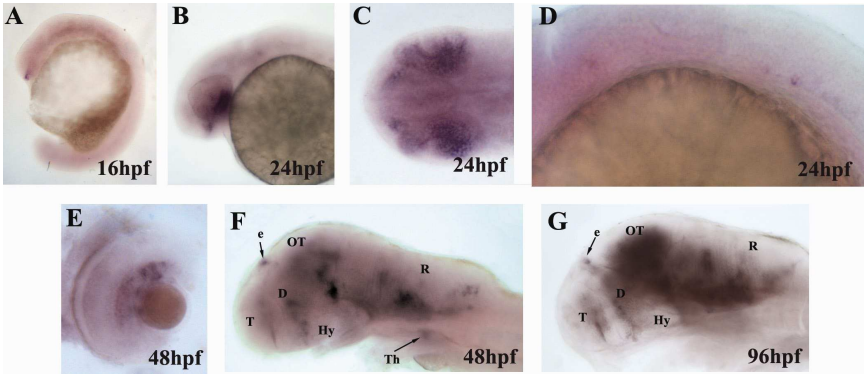

Figure. 20. Whole mount *in situ* hybridization on zebrafish embryo for *rxfp3-2*a transcript during embryogenesis. Embryo at different developmental stage detected with *rxfp3-2*a riboprobes (A-G). Lateral view of somitogenesis stage (A). Lateral (B) and dorsal view (C) of early pharyngula stage. Lateral view of magnification of rhomboencephalic region at early pharyngula stage (D). Magnification of zebrafish eye at late pharyngula stage (E). Lateral view of flat mounted brain region at pharyngula stage (F). Black arrow indicates e: epiphysis and Th: thymus. lateral view of flat mounted brain region at larva stage (G). Black arrow indicates e: epiphysis. D: diencephalon; e: epiphysis; Hy: hypothalamus; OT: optic tectum; R: rhomboencephalon; T: telencephalon.

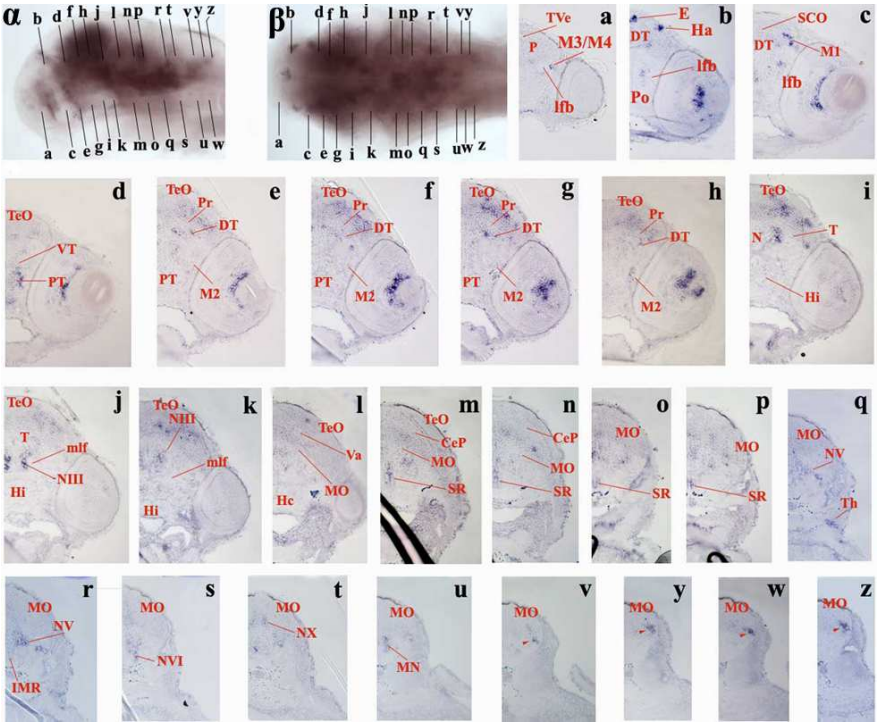

Figure. 21. **Whole mount *in situ* hybridization at 96 hpf lateral view (α), dorsal view (β).** Trasversal section of whole mount *in situ* hybridization at 96 hpf zebrafish embryo. Red arrow indicates a cell cluster likely representing M3 (entopeduncular migrated complex) or M4 (telencephalic migrated area). Red arrowheads indicate row cells in the medulla oblongata; CeP, cerebellar plate; DT, dorsal thalamus; E, ephiphysis; Ha, habenula; Hc, caudal hypothalamus; Hi, intermediate hypothalamus; lfb, lateral forebrain bundle; IMR, intermediate raphè; M1, migrated pretectal area; M2, migrated posterior tuberculum area; M4, telencephalic migrated area; mlf, medial longitudinal fascicle; MN, spinal motor neurons; MO, medulla oblongata; N, region of the nucleus of medial longitudinal fascicle; NIII, oculomotor nerve nucleus; NV, NVI, NX, nuclei of cranial nerves; P, motor nuclei of pallium; Po, preoptic region; Pr, pretectum; PT, posterior tuberculum; SCO, subcommissural organ; SR, superior

raphè; T, midbrain tegmentum; TeO, optic tectum; Th, thymus; TVe, telencephalic ventricle; Va, valvula cerebelli; VT, ventral thalamus.

Regarding to *rxfp3-3*b, from fertilized eggs to somitogenesis, we revealed faint and broadly distributed hybridization signal (data not shown). At early pharyngula stage (24 hpf), we observed a restricted signal in ventral retina (Figure. 22A). Lately, at 48 hpf, a specific signal was revealed in the mesencephalic region (Figure. 22B, C). At early larval stage (72 hpf), the gene expression was observed in the epiphysis (Figure 22D) and in some scattered cells in the rhomboencephalon (Figure. 22I). Moreover, at larval stage, other expression territories were localized in the raphè, hypothalamus (Figure. 22C, E). In order to better characterize the expression territories, we performed transverse sections of the hybridized embryos at 96 hpf (Figure. 23A). Sections of the head region evidenced the expression in the retinal cells, in particular, in the ganglion cell layer (Figure. 23B). In the brain region, particularly evident is the expression in the ventral thalamus, optic tectum, M2, (Figure 23B, C) and more caudally, in the putative periaqueductal gray (PAG), the putative nucleus incertus, the raphè and hyphothalamus (Figure. 23D, E, F.). In addiction, transverse sections evidenced *rxfp3-3*b expression in the pancreas (Figure. 23I).

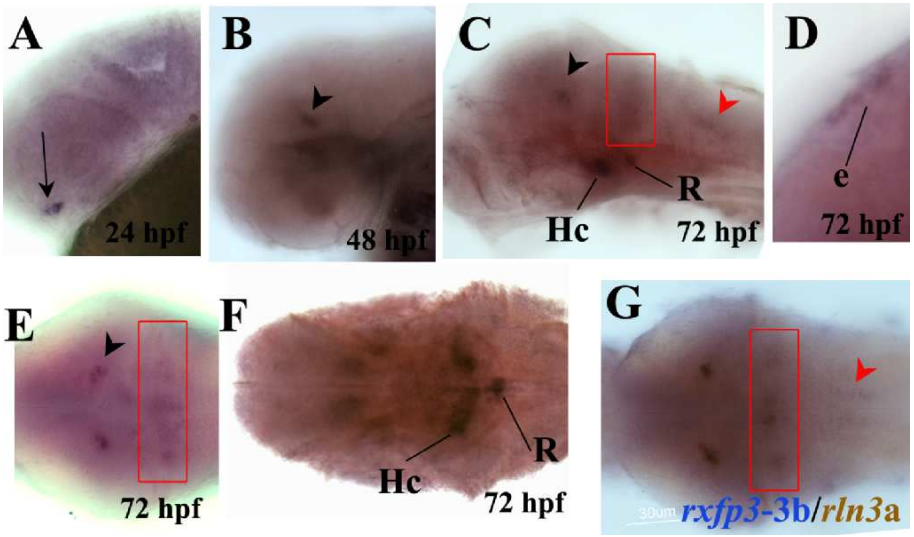

Figure. 22. **Whole mount *in situ* hybridization for *rxfp3-3*b at different developmental stage as indicated in the panel**. Lateral view of embryo at early pharyngula stage (A). Dorsal lateral view of embryo at late pharyngula stage (B). Embryo at early larval stage (C). Magnification of epiphysis region of embryo at early larval stage (D). Ventral view of embryo at early larval stage (E). Double *in situ* hybridization for *rln3*a transcript (blue signal) and *rxfp3-2*b transcript (orange signal) dorsal view at late larval stage (F). Black arrow indicates retina, black arrowhead indicates periacqueductal gray, red arrowhead indicates romboencephalic region. In the red rectangle is indicated the nucleus incertus. e, epiphysis; Hc, caudal hypothalamus; R, raphè.

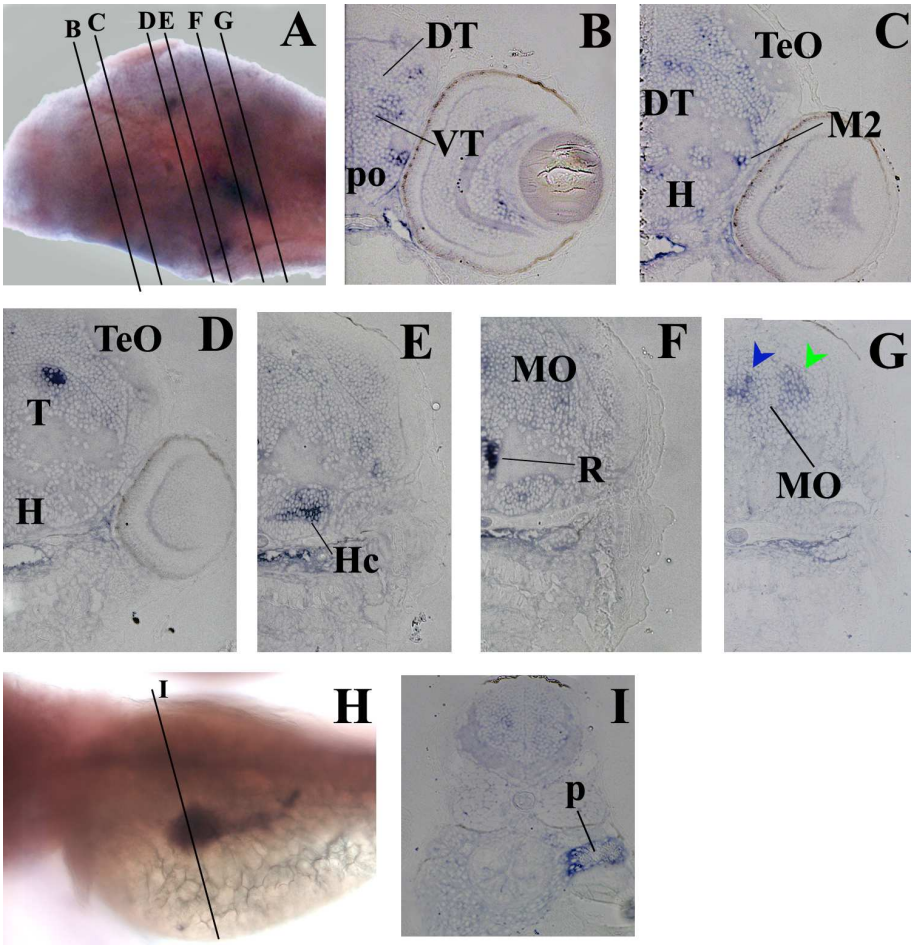

Figure. 23. **Whole mount *in situ* hybridization at 96 hpf.** Lateral view (A), dorsal view for *rxfp3-3b* transcript (H) of embryo at 96 hpf. The trasversal section along the embryo at 96 hpf is indicated (A, whole brain lateral view) and lateral view of 96 hpf zebrafish embryo trunck region (H). Blue arrowhead indicates nucleus incertus, green arrowhead indicates DT, dorsal thalamus; H: hypothalamus; Hc, caudal hypothalamus; M2, migrated posterior tuberculum area; MO, medulla oblongata; NI, nucleus incertus; p, pancreas; PAG, periaqueductal gray; po, preoptic area; R, raphè; T, tegmental nucleus; TeO, optic tectum; VT, ventral thalamus.

5.0 CONCLUSION

Relaxin ligand/receptor system has been widely studied in mammalian adult organisms. This molecular system is involved in many physiological functions ranging from reproduction to neuroendocrine system. In particular, RLN has been mainly linked to reproduction, although many studies evidenced its involvement in other physiological contexts since, among the expression and target tissues, there are the brain, kidney, heart, liver, and pancreas. For INSL3 and INSL5, it has been clearly defined their roles in reproduction and gastrointestinal system respectively (Adham et al., 1993, Conklin et al., 1999). The most recently identified family member, the RLN3, has been characterized as a neuropeptide involved in stress and metabolic control (Bathgate et al., 2002; 2013). All the relaxin peptides exert their physiological effects by interacting and activating 4 GPCR receptors [relaxin family peptide receptors 1–4 (RXFP1–4)]. Few studies have been performed on the relaxin/receptor system during embryonic development and in vertebrate models beyond mammals. In the present thesis, I reported, the identification, cloning and characterization of relaxin ligand/receptor genes in the zebrafish experimental model. In particular, my experimental analysis was carried out during embryonic development. Recent evolutionary analyses revealed that vertebrate RLN/INSL genes and their receptors primarily diversified through the two rounds (2R) of whole genome duplication (WGD), that occurred in early vertebrate evolution (Good et al., 2012). In addition, the third whole teleost fish-specific WGD (3R), further contributed to the current number of fish genes (Good et al., 2012). As I reported in the introduction section, zebrafish genome contains 6 relaxin ligand and 11 relaxin receptor genes (Figure. 2, 3). Our previous results already highlighted the powerful of zebrafish model for the relaxin ligand/receptor molecular characterization. The *rln3*a/b gene expression pattern analysis showed both conserved and divergent features compared to the corresponding mammalian homologues. Taken overall, the experimental data supported the idea of an ancestral function of *Rln3* peptide as a neurotransmitter, and provided the first evidence of the existence of the neural territory known as nucleus incertus (NI) in fish (Donizetti et al., 2008, 2009). In order to extend the knowledge on relaxin system, in particular on

its involvement in embryonic development, the present thesis focused on the other zebrafish relaxin ligands and the cognate receptors. In the present work, a preliminary analysis was performed to identify coding region for two genes, *rln* and *rxfp1*, which lacked in literature and in public nucleotide databases. Analysis of the identified *rln* sequence showed interesting evolutionary features. Overall, the zebrafish mature Rln amino acid sequence (made of B and A peptides) showed higher similarity to the zebrafish Rln3a, Rln3b and human RLN3, than to the homologue mammalian RLN. This reflects the common evolutionary origin of that gene from a common ancestral RLN3-like gene. In addition, the comparison highlighted that during evolution zebrafish *rln* and *rln3* sequences remained more similar than mammalian RLN and RLN3, which showed greater sequence divergence (Hsu et al., 2003; Wilkinson et al., 2005; Wilkinson and Bathgate 2007). In more detail, B and A domains of zebrafish relaxin peptide evolved differently, in fact, B domain is more conserved than A domain. Taking into account that the A domain might contribute to ligand binding by orienting the B domain (Hossain et al., 2008; Park et al., 2008), the dissimilarity of zebrafish *Rln* A domain could reflect different binding specificity for the various relaxin receptors. My data corroborates the idea of a more complex ligand/receptor pairing scenario than previously imagined, in accordance with the data on the ability of the mammalian RXFP3 to interact with H3, H2 and INSL3 ligands transducing different metabolic pathways (van der Westhuizen et al., 2010). For what concerns the *rxfp1* gene, the general conservation of syntenic genomic organization, exon-intron structure, and of many amino acid residues important for ligand interaction and receptor functioning supported the hypothesis of the identification of the mammalian homologue of the zebrafish *rxfp1*.

The analysis of expression profile of relaxin ligands and receptors genes was initially performed by PCR analysis. Results (summarized in Table 3) showed that the relaxin/receptor system is active during zebrafish embryonic development. It is note of worth that some receptor genes are not expressed during embryogenesis, suggesting that they likely are required later in organism's life. Another interesting insight is that, when duplicated, the paralogue genes showed a different expression pattern, likely reflecting a diversification of their function after their separation during evolution.

	4 hpf	8 hpf	16 hpf	24 hpf	48 hpf	72 hpf
rln	X	X	X	X	X	X
rln3a	X		X	X	X	X
rln3b	X	X	X	X	X	X
insl5a				X	X	X
insl5b					X	X
rxfp1	X	X	X	X	X	X
rxfp2a						
rxfp2b						
rxfp2-like					X	X
rxfp3-1			X	X	X	X
rxfp3-2a		X	X	X	X	X
rxfp3-2b						X
rxfp3-3a1						X
rxfp3-3a2						
rxfp3-3a3						
rxfp3-3b	X	X	X	X	X	X

Table 3. **Summary of relaxin ligands and receptors embryonic expression pattern analysed by RT-PCR and qRT-PCR experiments.** The same colour indicates the paralogue genes. (the *rln3*a and *rln3*b expression data are provided by Donizetti et al., 2008, 2009).

Gene expression localization analysis was performed by means of in situ hybridization experiments and summarized in Table 4. Taken overall, my data show that relaxin peptides and their cognate receptors are mainly expressed in neuronal territories. These data further corroborate the hypothesis of an ancestral neuroendocrine function for the relaxin system. In addition, several non-neural territories are shown to express relaxin ligand and receptor genes.
The zebrafish *rln* gene expression pattern, in part, reflects the common evolutionary origin with *rln3*a. In fact, both are expressed in the putative zebrafish nucleus incertus, as a consequence of common inherited regulatory pathway. Differently, new expression territories have likely been acquired in *rln* expression pattern during evolutionary diversification of relaxin genes. Among these territories, the olfactory placode cells expressed the *rln* gene throughout embryogenesis. No expression in this territory was revealed in post-embryonic larvae, leading to the hypothesis of a function for the Rln in olfactory placode development. The *rln* gene expression was also revealed in the preoptic area and around the anterior commissure of the telencephalon, providing evidence of an involvement in the development and functioning of the visual system. Moreover the *rln* gene expression was also detected in thyroid and pancreas regions, which highlights a possible role as a paracrine and endocrine hormone. The expression pattern of zebrafish *rln* revealed that in comparison to rodents there are some expression territories in common between fish and mammals, both in the brain and in extraneural territories such as liver and pancreas (Ma et al., 2006; Halls et al., 2009; Burazin et al., 2005; Gunnersen et al., 1995). The *insl-5*a and *insl-5*b paralogue genes are expressed in intestine tissue during embryonic development. I demonstrated that in the adult zebrafish, these two genes specialized their expression pattern in different intestinal cell types. In particular, I revealed *insl-5*a transcript in the goblet cells, whose function is to secrete mucus. Differently, *insl-5*b is expressed in enteroendocrine cells (that are specialized endocrine cells of the gastrointestinal tract), which play critical roles in regulating gastrointestinal secreting hormones. Taken into account that in mouse and human, the INSL5 gene is expressed in the colon and is likely involved in the intestinal motility (Conklin et al., 1999),

my results show that this function has likely been established early in vertebrate evolution.
In order to understand the role of relaxins during embryogenesis, my analysis included gene expression pattern of their receptors. *Rxfp1,* which in mammals is the cognate receptor for RLN, is essentially expressed in the neural territories. Among them, branchial arch region and terminal nerve, which share a common origin from the neural crests. This might reflect a function of *rxfp1* in the early phases of development of such structures. The expression in the terminal nerve involves all the embryonic stages, reflecting, more probably, a role for the *rxfp1* receptor in the neuromodulatory function of the terminal nerve. I found gene expression in the epiphysis, or pineal gland, which, in non-mammalian vertebrates including zebrafish, contains light-sensitive photoreceptor and all the elements required for photic entrainment and circadian rhythm generation (Vatine, 2011). The expression of the *rxfp1* gene extends in other territories such as posterior tuberculum, preoptic region, optic tectum, involved in sensory process of the visual system. In addition the *rxfp1* gene is expressed in tegmentum/pons region, hindbrain and hypothalamus. The expression of *Rxfp1* receptor in all such neural territories suggests a role in different neural mechanisms such as somatosensory processing, neuroendocrine and autonomic regulation, as proposed for the homologue receptor in the adult rat brain (Ma et al., 2006). Zebrafish *rxfp2-like* gene (the mammalian homologue is considered the cognate receptor for INSL3) is the only *rxfp2* paralogue gene expressed during embryonic development. The corresponding transcript is localized in the epiphysis, habenula and preoptic area. Also in rat brain there is high RXFP2 expression in the habenula and other territories such as thalamic nuclei, olfactory tubercle signalling system, which are involved in sensorimotor, limbic and cognitive functions (Sedaghat et al., 2008).
Among relaxins receptors, teleost *rxfp3*s show the greatest expansion in terms of orthologs and paralogs, since zebrafish genome possess 7 *rxfp3* genes. The *rxfp3-1* gene is expressed in the developing interrenal gland, the homologue of mammalian adrenocortical gland, where the mammalian RXFP3 gene is expressed. The interrenal/adrenal gland is a key element of the hypothalamic-pituitary-adrenal/interrenal axis that controls the stress response and regulates many body processes, including digestion, the immune

system, mood and emotions, sexuality and energy storage (Chan et al., 2008). In addition, zebrafish *rxfp3*-1 is expressed in the rhombencephalic region of larval brain.
The *rxfp3-2a* has shown the most complex expression pattern, in particular in the developing brain. The expression territories of zebrafish *rxfp3-2*a relates to neural structure involved in visual sensory perception and signal elaboration, leading to the idea of an involvement in the entire visual-motor system. Another interesting feature of the *rxfp3-2*a gene is the expression in habenular cells. The habenula is a neural structure involved in emotional behaviours which conveys neural information from the limbic forebrain to the nuclei in the ventral midbrain and hindbrain (such as raphè and nucleus incertus in mammals and griseum centrale in fishes) in a pathway which is conserved throughout the vertebrate evolution (Okamoto, 2012). Moreover, we observed the *rxfp3-2*a expression in the pineal gland. The *rxfp3-3*b gene expression pattern also offers some interesting discussion items. In fact, zebrafish *rxfp3-3*b shares with mammalian RXFP3 the expression in some brain areas. Among them, the periaqueductal gray, which is involved in pain analgesia, fear, anxiety, vocalization (Olango et al., 2012; Sugiyama et al., 2010., Smith et al., 2011); in raphè, which is involved in the control of chronic social defeat stress (CSDS), depression, and anxiety (Boyarskikh et al., 2013; Rozeske et al., 2011; Smith et al., 2011); in the hypothalamus, which is involved in different neural processes, among them the control of sleep and social behaviour. In addition, among other neural territories, I revealed the expression in the putative zebrafish nucleus incertus, which, as aforementioned is a key element for arousal (sleep/wakefulness), stress reponses, and learning and memory; and is involved in the pathology of related psychiatric diseases such as insomnia, anxiety and depression, and cognitive deficits (Ryan et al., 2011). The *rxfp3-3*b expression was also revealed in the pancreatic region. Overall, the regions where we detected zebrafish *rxfp3* paralogue genes expression (both neural and non-neural) are mostly overlapping with the mammalian homologue gene. It has often been argued that gene-duplication events are more commonly followed by subfunctionalization than neofunctionalization event leading to the duplicate-genes preservation. Indeed, the subfunctionalization process may facilitate such evolution by preserving gene duplicates and maintaining their exposure to natural selection and/or by removing

pleiotropic constraints (Lynch and Force., 2000). My data seem in agreement with such hypothesis where the subfunctionalization events for the zebrafish *rxfp3* genes in part recapitulated the expression, and probably the function, of the mammalian RXFP3 and RXFP4 genes.
In conclusion, taken into account that several territories of relaxins and receptors gene expression are shared between mammals and zebrafish, it is possible to hypothesize that also in fish they may have many physiological effects involving olfactory system, vision system, arousal system, circadian rhythm, fear, learning, memory, feeding, stress and metabolism. In addition, it is worth of note that, since that genes are expressed during embryonic development, their functions are established very early in the organism's life.

	16 hpf		24 hpf		48 hpf		72 hpf		96 hpf	
	ligand	receptor	ligand	receptor	ligand	receptor	ligand	receptor	ligand	receptor
BRAIN	rln3a, rln3b, rln	rxfp1, Rxfp3-2a	rln3a, rln3b, rln	rxfp1, Rxfp3-2a	rln3a, rln3b, rln	rxfp1, Rxfp3-2a, Rxfp3-3b, Rxfp2-4	rln3a, rln3b, rln	rxfp1, Rxfp3-2a, Rxfp3-3b, Rxfp2-4, Rxfp3-1	rln3a, rln3b, rln	rxfp1, Rxfp3-2a, Rxfp3-3b, Rxfp2-4, Rxfp3-1
RETINA			Rxfp3-2a, Rxfp3-3b		Rxfp3-2a		Rxfp3-2a, Rxfp2-4		Rxfp3-2a, Rxfp2-4, Rxfp3-3b	
PANCREAS							rln, insl5a		rln, Rxfp3-3b	
THYMUS					Rxfp3-2a		Rxfp3-2a		Rxfp3-2a	
INTESTINE							insl5a		insl5a, insl5b	
ADRENAL GLAND			Rxfp3-1		Rxfp3-1					
THYROID									rln	
OLFACTORY PLACODE			rln		rln		rln		rln	
Terminal nerve			rxfp1		rxfp1		rxfp1		rxfp1	

Table 4. **Summary of relaxin ligands and their cognate receptors expression territories.** Summary of expression territories by *in situ* hybridization, during zebrafish developmental stage.

6.0 REFERENCES

Abi-Rached, L., Gilles, A., Shiina, T., Pontarotti, P., Inoko, H. 2002. Evidence of en bloc duplication in vertebrate genomes. Nat Genet. 31, 100-105.

Adham, IM., Burkhardt, E., Benahmed, M., Engel, W. 1993. Cloning of a cDNA for a novel insulin-like peptide of the testicular Leydig cells. J Biol Chem. 268: 26668–26672.

Anand-Ivell, R., Heng, K., Hafen, B., Setchell, B., Ivell, R. 2009. Dynamics of INSL3 peptide expression in the rodent testis. Biol Reprod. 81, 480-7.

Anand-Ivell, RJ., Relan, V., Balvers, M., Coiffec-Dorval, I., Fritsch, M., Bathgate, RA., Ivell, R. 2006. Expression of the insulin-like peptide 3 (INSL3) hormone-receptor (LGR8) system in the testis. Biol Reprod. 74, 945–953.

Arroyo, JI., Hoffmann, FG., Opazo, JC. 2012. Gene turnover and differential retention in the relaxin/insulin-like gene family in primates. Mol Phylogenet Evol. 63, 768-76.

Bathgate, R. A. D., Halls, M. L., van der Westhuizen, E.T., Callander, G. E., Kocan, M., Summers. R. J. 2013. Relaxin family peptide and their receptors. Physiol Rev. 93, 405–480.

Bathgate, RA, Ivell, R, Sanborn, BM, Sherwood, OD, Summers, RJ. 2006. International Union of Pharmacology LVII: Recommendations for the nomenclature of receptors for relaxin family peptides. Pharmacol Rev. 58, 7–31.

Bathgate, RA, Samuel, CS, Burazin, TC, Layfield, S, Claasz, AA, Reytomas, IG, Dawson, NF., Zhao, C., Bond, C., Summers, RJ., Parry, LJ., Wade, JD., Tregear, GW. 2002b. Human relaxin gene 3 (H3) and the equivalent mouse relaxin (M3) gene. Novel members of the relaxin peptide family. J Biol Chem. 277, 1148-57.

Bathgate, RA., Siebel, AL., Tovote, P., Claasz, A., Macris, M., Tregear, GW., Parry, LJ. 2002. Purification and characterization of relaxin from the tammar wallaby (Macropus eugenii): bioactivity and expression in the corpus luteum. Biol Reprod. 67, 293-300.

Bathgate, RAD., Hsueh, AJW., Sherwood, OD. Physiology and molecular biology of the relaxin peptide family. In: Knobil and Neill's Physiology of Reproduction, edited by Neill JD. New York: Academic, 2006.

Boels, K., Hermans-Borgmeyer, I., Schaller, HC. 2004. Identification of a mouse orthologue of the G-protein-coupled receptor SALPR and its expression in adult mouse brain and during development. Brain Res Dev Brain Res. 152, 265–268.

Bogatcheva, NV., Truong, A., Feng, S., Engel, W., Adham, IM., Agoulnik, AI. 2003. GREAT/LGR8 is the only receptor for insulin-like 3 peptide. Mol Endocrinol. 17, 2639–2646.

Boyarskikh, UA., Bondar, NP., Filipenko, ML., Kudryavtseva, NN. 2013. Downregulation of Serotonergic Gene Expression in the Raphe Nuclei of the Midbrain Under Chronic Social Defeat Stress in Male Mice. Mol Neurobiol. DOI 10.1007/s12035-013-8413

Brailoiu, E., Dun, SL., Gao, X., Brailoiu, GC., Li, JG., Luo, JJ., Yang, J., Chang, JK., Liu-Chen, LY., Dun, NJ. 2009. C-peptide of preproinsulin-like peptide 7: localization in the rat brain and activity in vitro. Eugen Neuroscience. 159, 492–500.

Büllesbach, EE., Schwabe, C. 2000. The relaxin receptor-binding site geometry suggests a novel gripping mode of interaction. J Biol Chem. 275, 35276-35280.

Burazin, TC., Bathgate, RA., Macris, M., Layfield, S., Gundlach, AL., Tregear, GW. 2002. Restricted, but abundant, expression of the novel rat gene-3 (R3) relaxin in the dorsal tegmental region of brain. J Neurochem. 82, 1553–1557.

Burazin, TC., Johnson, KJ., Ma, S., Bathgate, RA., Tregear, GW., Gundlach, AL. 2005. Localization of LGR7 (relaxin receptor) mRNA and protein in rat forebrain: correlation with relaxin binding site distribution. Ann NY Acad Sci. 1041, 205–210.

Callander, GE., Bathgate, RA. 2010. Relaxin family peptide systems and the central nervous system. Cell Mol Life Sci. 67, 2327–2341.

Conklin, D., Lofton-Day, CE., Haldeman, BA., Ching, A., Whitmore, TE., Lok, S., Jaspers, S. 1999. Identification of INSL5, a new member of the insulin superfamily. Genomics. 60, 50– 56.

Dehal, P., Boore, JL. 2005. Two rounds of whole genome duplication in the ancestral vertebrate. PLoS Biol. 3:e314.

Denver, RJ. 2009. Structural and functional evolution of vertebrate neuroendocrine stress systems. Ann N Y Acad Sci. 1163, 1-16.

Donizetti, A., Grossi, M., Pariante, P., D'Aniello, E., Izzo, G., Minucci, S., Aniello, F. 2008. Two neuron clusters in the stem of postembryonic zebrafish brain specifically express relaxin-3 gene: first evidence of nucleus incertus in fish. Dev Dyn. 237, 3864–3869.

Donizetti, A., Fiengo, M., del Gaudio, R., Di Giaimo, R., Minucci, S, Aniello, F. 2010. Characterization and developmental expression pattern of the relaxin receptor rxfp1 gene in zebrafish. Dev. Growth Differ. 52, 799–806.

Donizetti, A., Fiengo, M., Minucci, S. & Aniello, F. 2009. Duplicated zebrafish relaxin-3 gene shows a different expression pattern from that of the co-orthologue gene. Dev. Growth Differ. 51, 715–722.

Fiengo, M., Donizetti, A., Del Gaudio, R., Minucci, S., Aniello, F. 2012. Characterization, cDNA cloning and expression pattern of relaxin gene during embryogenesis of Danio rerio. Develop. Growth Differ. 54, 579-587.

Fredriksson, R., Höglund, PJ., Gloriam, DE., Lagerström, MC., Schiöth, H. B. 2003. Seven evolutionarily conserved human rhodopsin G protein-coupled receptors lacking close relatives. FEBS Lett. 554, 381-388.

Gloriam, DE., Foord, SM., Blaney, FE., Garland, SL. J. 2009. Definition of the G protein-coupled receptor transmembrane bundle binding pocket and calculation of receptor similarities for drug design. Med Chem. 52, 4429-4442.

Good, S., Yegorov, S., Martijn, J., Franck, J., Bogerd, J. 2012. New insights into ligand-receptor pairing and coevolution of relaxin family peptides and their receptors in teleosts. Int J Evol Biol. 310278.

Good-Avila, V S., Yegorov, S., Harron, S., Bogerd, J., Glen, P., Ozon, J and Brian, C Wilson. 2009. Relaxin gene family in teleosts: phylogeny, syntenic mapping, selective constraint, and expression analysis. BMC Evolutionary Biology. 9, 293.

Gorlov, IP., Kamat, A., Bogatcheva, NV., Jones, E., Lamb, DJ., Truong, A., Bishop, CE., Mc- Elreavey, K., Agoulnik, AI. 2002. Mutations of the GREAT gene cause cryptorchidism. Hum Mol Genet. 11, 2309–2318.

Goto, M., Swanson, LW., Canteras, NS. 2001. Connections of the nucleus incertus. J Comp Neurol. 438, 86–122.

Goujon, M., McWilliam, H., Li, W., Valentin, F., Squizzato, S., Paern, J. & Lopez, R. 2010. A new bioinformatics analysis tools framework at EMBL-EBI. Nucleic Acids Res. 38, 695– 699.

Gunnersen, JM., Crawford, RJ., Tregear, GW. 1995. Expression of the relaxin gene in rat tissues. Mol Cell Endo. 110, 55–64.

Halls, ML., Cooper, DM. 2010. Sub-picomolar relaxin signaling by a pre-assembled RXFP1, AKAP79, AC2, beta-arrestin 2, PDE4D3 complex. EMBO J. 29, 2772–2787.

Halls, ML., van der Westhuizen, ET., Bathgate, RA., Summers, RJ. 2007. Relaxin family peptide receptors–former orphans reunite with their parent ligands to activate multiple signaling pathways. Br J Pharmacol. 150, 677–691.

Halls, ML., van der Westhuizen, ET., Bathgate, RAD and Summers, RJ. 2007. Relaxin Family Peptide Receptors–former orphans reunite with their parent ligands to activate multiple signalling pathways. British Journal of Pharmacology. 150, 677–691.

Haugaard-Jonsson, LM., Hossain, MA., Daly, NL., Craik, DJ., Wade, JD., Rosengren, KJ. 2009. Structure of human insulin-like peptide 5 and characterization of conserved hydrogen bonds and electrostatic interactions within the relaxin framework. Biochem J. 419, 619–627.

Hida, T., Takahashi, E., Shikata, K., Hirohashi, T., Sawai, T., Seiki, T., Tanaka, H., Kawai, T., Ito, O., Arai, T., Yokoi, A., Hirakawa, T., Ogura, H., Nagasu, T., Miyamoto, N., Kuromitsu, J. 2006. Chronic intracerebroventricular administration of relaxin-3 increases body weight in rats. J Recept Signal Transduct Res. 26, 147-58.

Hisaw, FL. 1926. Experimental relaxation of the pubic ligament of the guinea pig. Proc Soc Exp Biol Med. 23, 661–663.

Hoegg, S., Brinkmann, H., Taylor, JS., Meyer, A. 2004. Phylogenetic timing of the fish-specific genome duplication correlates with the diversification of teleost fish. J Mol Evol. 59, 190-203.

Hossain, MA., Rosengren, KJ., Haugaard-Jonsson, LM., Zhang, S., Layfield, S., Ferraro, T., Daly, NL., Tregear, GW., Wade, JD., Bathgate, RA. 2008. The A-chain of human relaxin family peptides has distinct roles in the binding and activation of the different relaxin family peptide receptors. J Biol Chem. 283, 17287–17297.

Hsu, SY., Nakabayashi, K., Nishi, S., Kumagai, J., Kudo, M., Sherwood, OD., Hsueh, AJ. 2002. Activation of orphan receptors by the hormone relaxin. Science. 295, 671–674.

Hsu, SY., Semyonov, J., Park, JI., Chang, CL. 2005. Evolution of the signaling system in relaxin-family peptides. Ann N Y Acad Sci. 1041, 520-529.

Hsu, SY., Semyonov, J., Park, JI., Chang, CL. 2005. Evolution of the signaling system in relaxinfamily peptides. Ann NY Acad Sci. 1041, 520–529,

Hsu, SYT. 2003. New insights into the evolution of the relaxin-LGR signaling system. Trends Endocrinol Metab. 14, 303–309,

Ivell, R., Einspanier, A. 2002. Relaxin peptides are new global players. Trends Endocrinol Metab. 13, 343–348.

Ivell, R., Kotula-Balak, M., Glynn, D., Heng, K., Anand-Ivell, R. 2011. Relaxin family peptides in the male reproductive system–a critical appraisal. Mol Hum Reprod. 17, 71–84.

Kawamura, K., Kumagai, J., Sudo, S., Chun, SY., Pisarska, M., Morita, H., Toppari, J., Fu, P., Wade, JD., Bathgate, RA., Hsueh, AJ. 2004. Paracrine regulation of mammalian oocyte maturation and male germ cell survival. Proc Natl Acad Sci USA. 101, 7323–7328.

Kimmel, C. B., Ballard, W. W., Kimmel, S. R., Ullmann, B. Shilling, T. F. 1995. Stages of embryonic development of the zebrafish. Dev. Dyn. 203, 253–310.

Krajnc-Franken, MA., van Disseldorp, AJ., Koenders, JE., Mosselman, S., van Duin, M., Gossen, JA. 2004. Impaired nipple development and parturition in LGR7 knockout mice. Mol Cell Biol. 24, 687–696.

Kubota, Y., Temelcos, C., Bathgate, RA., Smith, KJ., Scott, D., Zhao, C., Hutson, JM. 2002. The role of insulin 3, testosterone, Mullerian inhibiting substance and relaxin in rat gubernacular growth. Mol Hum Reprod. 8, 900–905.

Kumagai, J., Hsu, SY., Matsumi, H., Roh, JS., Fu, P., Wade, JD., Bathgate, RA., Hsueh, AJ. 2002. INSL3/Leydig insulin-like peptide activates the LGR8 receptor important in testis descent. J Biol Chem. 277, 31283–31286.

Larkin, M.A., Blackshields, G., Brown, N.P., Chenna, R., McGettigan, P.A., McWilliam, H., Valentin, F., Wallace, I.M., Wilm, A., Lopez, R., Thompson, J.D., Gibson, T.J, Higgins, D.G. 2007. Clustal W and Clustal X version 2.0. Bioinformatics. 23, 2947–2948.

Liu, C., Chen, J., Kuei, C., Sutton, S., Nepomuceno, D., Bonaventure, P., Lovenberg, TW. 2005. Relaxin-3/insulin-like peptide 5 chimeric peptide, a selective ligand for G proteincoupled receptor (GPCR)135 and GPCR142 over leucine-rich repeat-containing G protein-coupled receptor 7. Mol Pharmacol. 67, 231–240.

Liu, C., Chen, J., Sutton, S., Roland, B., Kuei, C., Farmer, N., Sillard, R., Lovenberg, T. W. 2003. Identification of relaxin-3/INSL7 as a ligand for GPCR142. J Biol Chem. 278, 50765-50770.

Liu, C., Kuei, C., Sutton, S., Chen, J., Bonaventure, P., Wu, J., Nepomuceno, D., Kamme, F., Tran, DT., Zhu, J., Wilkinson, T., Bathgate, R., Eriste, E., Sillard, R., Lovenberg, TW. 2005. INSL5 is a high affinity specific agonist for GPCR142 (GPR100). J Biol Chem. 280, 292–300.

Luna, JJ., Riesewijk, A., Horcajadas, JA., de van Os, R., Dominguez, F., Mosselman, S., Pellicer, A., Simon, C. 2004. Gene expression pattern and

immunoreactive protein localization of LGR7 receptor in human endometrium throughout the menstrual cycle. Mol Hum Reprod. 10, 85–90.

Lynch, M., Force, A. 1999. The Probability of Duplicate Gene Preservation by Subfunctionalization. Department of Biology, University of Oregon, Eugene, Oregon 97403.

Ma, S., Bonaventure, P., Ferraro, T., Shen, PJ., Burazin, TC., Bathgate, RA., Liu, C., Tregear, GW., Sutton, SW., Gundlach, AL. 2007. Relaxin-3 in GABA projection neurons of nucleus incertus suggests widespread influence on forebrain circuits via G-protein-coupled receptor-135 in the rat. Neuroscience. 144, 165–190.

Ma, S., Shen, P. J., Sang, Q., Lanciego, J. L., Gundlach, A. L. (2009). Distribution of relaxin-3 mRNA and immunoreactivity and RXFP3- binding sites in the brain of the macaque, Macaca fascicularis. Ann N Y Acad Sci.1160, 256-258.

Ma, S., Shen, PJ., Burazin, TC., Tregear, GW., Gundlach, AL. 2006. Comparative localization of leucine-rich repeat-containing G-protein-coupled receptor-7 (RXFP1) mRNA and [33P]-relaxin binding sites in rat brain: restricted somatic co-expression a clue to relaxin action. Neuroscience. 141, 329–344.

Marriott, D., Gillece-Castro, B., Gorman, CM. 1992. Prohormone convertase 1 will process prorelaxin, a member of the insulin family of hormones. Mol Endocrinol. 6, 1441-1450.

Mazella, J., Tang, M., Tseng, L. 2004. Disparate effects of relaxin and TGFbeta1: relaxin increases, but TGFbeta1 inhibits, the relaxin receptor and the production of IGFBP-1 in human endometrial stromal/decidual cells. Hum Reprod. 19, 1513–1518.

McGowan, BM., Stanley, SA., Smith, KL., Minnion, JS., Donovan, J., Thompson, EL., Patterson, M., Connolly, MM., Abbott, CR., Small, CJ., Gardiner, JV., Ghatei, MA., Bloom, SR. 2006. Effects of acute and chronic relaxin-3 on food intake and energy expenditure in rats. Regul Pept. 136, 72–77.

McGowan, BM., Stanley, SA., Smith, KL., White, NE., Connolly, MM., Thompson, EL., Gardiner, JV., Murphy, KG., Ghatei, MA., Bloom, SR. 2005. Central relaxin-3 administration causes hyperphagia in male Wistar rats. Endocrinology. 146, 3295–3300.

Nef, S., Parada, LF. 1999. Cryptorchidism in mice mutant for INSL3. Nat Genet. 22, 295–299.

Okamoto, H., Agetsuma, M., Aizawa, H. 2012. Genetic dissection of the zebrafish habenula, a possible switching board for selection of behavioral strategy to cope with fear and anxiety. Dev Neurobiol. 72, 386-94.

Olango, WM., Roche, M., Ford, GK., Harhen, B., Finn, DP. 2012. The endocannabinoid system in the rat dorsolateral periaqueductal grey mediates fear-conditioned analgesia and controls fear expression in the presence of nociceptive tone. Br J Pharmacol. 65, 2549-2560.

Olinski, RP., Dahlberg, C., Thorndyke, M., Hallböök, F. 2006b. Three insulin-relaxin-like genes in Ciona intestinalis. Peptides. 27, 2535-2546.

Olinski, RP., Lundin, LG., Hallböök, F. 2006a. Conserved synteny between the Ciona genome and human paralogons identifies large duplication events in the molecular evolution of the insulinrelaxin gene family. Mol Biol Evol. 23, 10-22.

Olucha-Bordonau, F. E., Otero-García, M., Sánchez-Pérez, A. M., Núñez, A., Ma, S., Gundlach, A. L. 2012. Distribution and targets of the relaxin-3 innervation of the septal area in the rat. J Comp Neurol. 520, 1903-1939.

Overbeek, PA., Gorlov, IP., Sutherland, RW., Houston, JB., Harrison, WR., Boettger-Tong, HL, Bishop, CE., Agoulnik, AI. 2001. A transgenic insertion causing cryptorchidism in mice. Genesis. 30, 26–35.

Overbeek, PA., Gorlov, IP., Sutherland, RW., Houston, JB., Harrison, WR., Boettger-Tong HL, Bishop CE, Agoulnik AI. 2001. A transgenic insertion causing cryptorchidism in mice. Genesis. 30, 26–35.

Park, JI., Semyonov, J., Yi, W., Chang, CL., Hsu, SY. 2008. Regulation of receptor signaling by relaxin A chain motifs: derivation of pan-specific and LGR7-specific human relaxin analogs. J Biol Chem. 283, 32099–32109.

Park, JI., Semyonov, J., Yi, W., Chang, CL., Hsu, SY. 2008. Regulation of receptor signaling by relaxin A chain motifs: derivation of pan-specific and LGR7-specific human relaxin analogs. J Biol Chem. 283, 32099–32109.

Richard, Ivell., Kotula-Balak, M., Glynn, D., Heng, K., Anand-Ivell, R. 2011. Relaxin family peptides in the male reproductive system—a critical appraisal Molecular. Human Reproductio. 17, 71–84.

Konga, R C.K., Shilling P J., Lobb, D K., Gooley, P R., Bathgate, R A.D. 2010. Membrane receptors: Structure and function of the relaxin family peptide receptors, Molecular and Cellular Endocrinology. 320, 1–15.

Rozeske, RR., Evans, AK., Frank, MG., Watkins, LR., Lowry, CA., Maier, SF.2011. Uncontrollable, but not controllable, stress desensitizes 5-HT1A receptors in the dorsal raphe nucleus. J Neurosci. 31, 14107-15.

Ryan, PJ., Ma, S., Olucha-Bordonau, FE., Gundlach, AL. 2011. Nucleus incertus--an emerging modulatory role in arousal, stress and memory. Neurosci Biobehav Rev. 35, 1326-41.

Scott, DJ., Layfield, S., Riesewijk, A., Morita, H., Tregear, GW., Bathgate, RA. 2004. Identification and characterization of the mouse and rat relaxin receptors as the novel orthologues of human leucine-rich repeat-containing G-protein-coupled receptor 7. Clin Exp Pharmacol Physiol. 31, 828–832.

Sedaghat, K., Shen, PJ., Finkelstein, DI., Henderson, JM., Gundlach, AL. 2008. Leucine-rich repeat-containing G-protein-coupled receptor 8 in the rat brain: Enrichment in thalamic neurons and their efferent projections. Neuroscience. 156, 319-33.

Sherwood, O.D. et al. (1984) Dynamic changes of multiple forms of serum immunoreactive relaxin during pregnancy in the rat. Endocrinology. 114, 806–813.

Smith, CM., Ryan, PJ., Hosken, IT., Ma, S., Gundlach, AL. 2011. Relaxin-3 systems in the brain-The first 10 years. J Chem Neuroanat. 42, 262–275.

Smith, CM., Shen, PJ., Banerjee, A., Bonaventure, P., Ma, S., Bathgate, RA., Sutton, SW., Gundlach, AL. 2010. Distribution of relaxin-3 and RXFP3 within arousal, stress, affective, and cognitive circuits of mouse brain. J Comp Neurol. 518, 4016–4045.

Sugiyama, Y., Shiba, K., Nakazawa, K., Suzuki, T., Hisa, Y. 2010. Brainstem vocalization area in guinea pigs. Neurosci Res. 66, 359-65.

Tanaka, M., Iijima, N., Miyamoto, Y., Fukusumi, S., Itoh, Y., Ozawa, H., Ibata, Y. 2005. Neurons expressing relaxin 3/INSL 7 in the nucleus incertus respond to stress. Eur J Neurosci. 21, 1659–1670.

Thisse, B., Heyer, V., Lux, A., Alunni, A., Degrave, A., Seiliez, I., Kirchner, J., Parkhill, J. P., Thisse, C. 2004. Spatial and temporal expression of the zebrafish genome by large-scale in situ hybridization screening. Methods Cell Biol. 77, 505–519.

Untergasser, A., Nijveen, H., Rao, X., Bisseling, T., Geurts, R. & Leunissen, J.A. 2007. Primer3Plus, an enhanced web interfaceto Primer3. Nucleic Acids Res. 35, W71–W74.

Van der Westhuizen, ET., Christopoulos, A., Sexton, PM., Wade, JD., Summers, RJ. 2010. H2 relaxin is a biased ligand relative to H3 relaxin at the relaxin family peptide receptor 3 (RXFP3). Mol Pharmacol. 77, 759–772.

Vatine, G., Vallone, D., Gothilf, Y., Foulkes, NS. 2011. It's time to swim! Zebrafish and the circadian clock. FEBS Lett. 585, 1485-1494.

Westerfield, M. 1995. The Zebrafish Book, University of Oregon Press, Eugene, OR.

Wilkinson, TN., Speed, TP., Tregear, GW., Bathgate, RA. 2005. Evolution of the relaxin-like peptide family. BMC Evol Biol. 12, 5-14.

Wilkinson, TN., Speed, TP., Tregear, GW., Bathgate, RA. 2005. Evolution of the relaxin-like peptide family. BMC Evol Biol. 5, 14.

Yegorov, S., Good, S. 2012 . Using paleogenomics to study the evolution of gene families: origin and duplication history of the relaxin family hormones and their receptors. PLoS One.7:e32923. doi: 10.1371.

Zimmermann, S., Steding, G., Emmen, JM., Brinkmann, AO., Nayernia, K., Holstein, AF., Engel, W., Adham, IM. 1999. Targeted disruption of the INSL3 gene causes bilateral cryptorchidism. Mol Endocrinol. 13, 681–691,